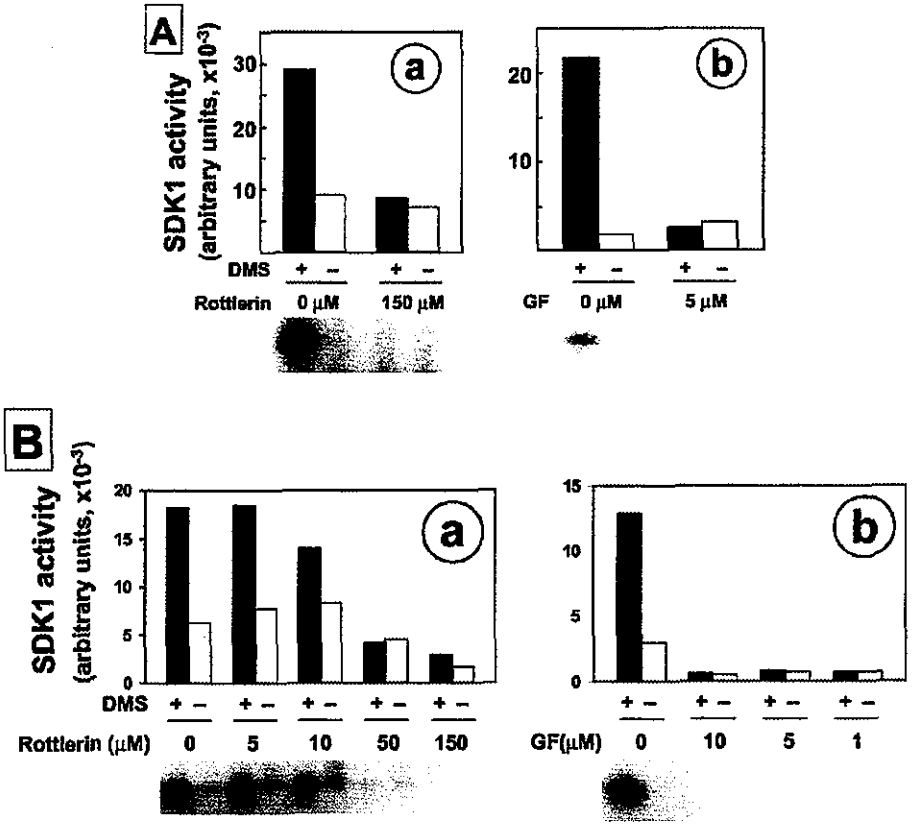

FIG. 5. **SDK1 activities of the rat liver fraction and of caspase-3-treated PKCδ and its inhibition by the PKC inhibitors rottlerin and GF109203X.** *A*, the rat liver fraction from the Mono Q step (Fig. 1*E*) containing the ~40-kDa protein was subjected to SDK1 activity assay, and this activity was tested for inhibition by 150 μM rottlerin (*panel a*) and 5 μM GF109203X (*GF*; *panel b*). A 4-μl sample was used for phosphorylation of 1 μg of 14-3-3β in the absence (−) or presence (+) of DMS. *B*, human recombinant PKCδ and caspase-3-treated PKCδ were subjected to SDK1 activity assay, and the activity was tested for dose-dependent inhibition by rottlerin (*panel a*) and GF109203X (*panel b*). Quantities of the inhibitor and the absence (−) or presence (+) of DMS are indicated on the *abscissa*. Quantities of PKCδ and caspase-3 were the same as described in the legends of Figs. 2*B* and 4. The bar graphs in *A* and *B* show the SDK1 activities in the presence (+; *black bars*) and absence (−; *white bars*) of DMS. In *A* and *B*, data from one of two experiments with very similar results are shown.

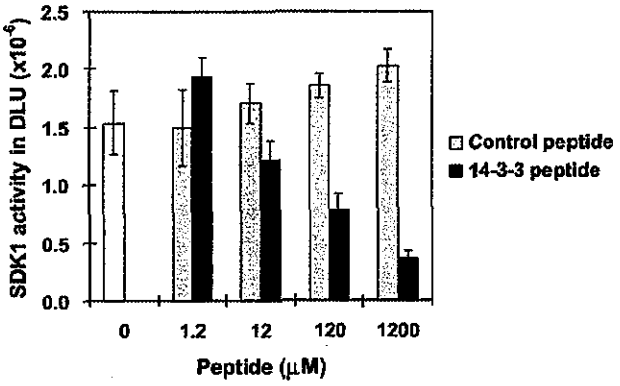

FIG. 6. **Inhibitory effect of the 14-3-3β icosapeptide on the SDK1 activity of caspase-3-treated PKCδ.** The SDK1 activity of caspase-3-treated PKCδ (quantities of PKCδ and caspase-3 as described in the legends of Figs. 2*B* and 4) was determined in the presence of various concentrations (*abscissa*) of the 14-3-3β icosapeptide (YKNV-VGARRSSWRVISSIEQ) and the control peptide (17 amino acids) as described under "Inhibition of the SDK1 Activity of Caspase-3-treated PKCδ by the 14-3-3 Peptide." SDK1 activity in the presence of the 14-3-3β icosapeptide (*black bars*) was strongly inhibited, whereas the control peptide (*gray bars*) had no effect. Values are the means of triplicate experiment; S.D. values are shown by the *error bars*.

strict structural requirements) indicate that the effect of Sph and DMS on SDK1 is physiological, in analogy to other specific lipid effects on signal transducer molecules.

The substrate specificity of SDK1 for 14-3-3 with a defined peptide sequence is indicated by the inhibition of SDK1 activity by the icosapeptide in the helix 3 domain. The kinase activities of both SDK1 and PKCδ may share the same ATP-binding site and "Ser/Thr kinase signature" (Table II) because both kinase activities are inhibited by common PKC inhibitors.

Sph has been suggested to be a "second messenger" because its low level is greatly increased upon stimulation of cells, *e.g.* platelet-derived growth factor and insulin-like growth factor cause activation of ceramidase, which converts Cer to Sph and fatty acid (31, 32). An increase in Sph may be due in part to synthesis from serine and palmitoyl-CoA, the classic synthetic system for Sph (33), although *de novo* synthesis in response to cell stimulation has not been clarified. Treatment of HL-60 cells with phorbol ester increases Sph levels by 3-fold, whereby the cells differentiate into macrophages. Treatment of the same cells with exogenous Sph causes apoptosis (34). DMS is considered to be derived from Sph by methylation through *N*-methyltransferase (35). The chemical level of cellular Cer is much higher than that of Sph, and the level of DMS is much lower than that of Sph. For example, the quantities of Cer, Sph, Sph-1-P, and DMS in 1×10^6 HL-60 cells, determined by LC/MS analysis, were ~12.07 μg, 0.61 ng, 0.048 ng, and 2.49 pg, respectively (36). The low levels of Sph and DMS and their increase in response to stimulation of cells are consistent with the hypothesis that they function as second messengers.

Sph converted from Cer or synthesized *de novo* may be short-lived because it is readily converted to Cer or Sph-1-P. A minor

quantity of DMS, if synthesized, is inhibitory to Sph kinase (37) and is absolutely stable. Thus, Sph in combination with DMS may be an effective inducer of various kinases, including SDK1 as well as other SDKs (17) whose biochemical properties remain to be elucidated.

The substrates for SDK1 are 14-3-3 protein family members (16, 29). How phosphorylation of 14-3-3 proteins by SDK1 contributes to the Sph/DMS-mediated signaling pathway remains to be elucidated. However, identification of SDK1 as the catalytic domain of PKCδ raises several intriguing possibilities. It may help explain a role for Sph/SDK1 in promoting cell death signaling.

14-3-3 proteins normally form homo- or heterodimers through their N-terminal helical structure, which is required for many of their regulatory roles in cells. For example, an intact dimeric form of 14-3-3 is essential for functional association of 14-3-3 with Raf1 (38, 39). Phosphorylation of 14-3-3 in the dimer interface would be expected to interfere with its dimer formation, thus interfering with 14-3-3-mediated functions. Accumulating evidence suggests that 14-3-3 can promote cell survival through its interaction with multiple pro-apoptotic proteins such as Bad and Bax (40, 41). For example, pro-apoptotic Bad complexed with Bcl-2/Bcl-x neutralizes the anti-apoptotic Bcl-2/Bcl-x effect, leading to cell death. This neutralization effect is inhibited by binding of 14-3-3 to Bad (40). Thus, 14-3-3 binding to Bad blocks apoptosis. It has been demonstrated that the catalytic domain of PKCδ or the SDK1 protein is released from its full-length proenzyme under a variety of cell stress or death conditions by activated caspase-3 (42–44). It is conceivable that the released catalytic domain of PKCδ/SDK1 is stimulated by Sph/DMS, leading to phosphorylation of 14-3-3 in the dimer interface. We propose that such phosphorylation may interfere with its binding to diverse ligands and neutralizes its role in inhibition of cell death. It is possible that phosphorylation of 14-3-3 by SDK1 may lead to dissociation of 14-3-3 to Bad or Bax, allowing Bad or Bax to induce mitochondrial dysfunction and cell death. It may not be a coincidence that cleaved PKCδ has been shown to target mitochondria (45, 46). Extensive further study is needed to confirm the possibility that inhibition of dimer formation by SDK1 blocks such a pro-survival function of 14-3-3.

It is also significant that we are able to suggest a mechanism that may control the dimerization status of 14-3-3 proteins. The 14-3-3 family is composed of multifunctional regulatory proteins that can interact with >100 protein partners in cells. A general mode of 14-3-3 binding is controlled by phosphorylation of target proteins at a defined phosphoserine/phosphothreonine motif (18, 47, 48). However, it remains unclear how the function of 14-3-3 itself is regulated and what determines the target specificity. Reversible regulation of 14-3-3 dimerization through phosphorylation in the dimer interface may provide a mechanism by which 14-3-3 activity is controlled. Identification of SDK1 as a homolog of PKCδ defines a signaling pathway that may directly control the ability of 14-3-3 to bind and to affect the function of diverse cellular proteins.

Acknowledgments—We are greatly indebted to various scientists and other individuals who played important roles in this study: Dr. Thayer White (Cell Therapeutics Inc.) for procedural suggestions during large-scale purification of SDK1; Noriko Shindo, Reiko Mineki, and Hikari Taka (Central Laboratory of Medical Sciences, Juntendo University School of Medicine), who assisted K. M. with sequencing the protein from SDK1 active fractions; Dr. Kazuo Fujikawa for purification of SDK1 through a heparin-Sepharose column; Lixin Zhang (Cetek Corp.) and Romesh Subramanian (Department of Pharmacology, Emory University School of Medicine), who assisted in preparation of 14-3-3 proteins; Dr. Tomikazu Sasaki for donation of the 17-amino acid peptide; Stephen Anderson (Pacific Northwest Research Institute) for preparation of manuscript and figures; and Theresa Nguyen, Chris Calbero, Kelle Hammock, Dustin Huynh, Alisha Cutler, and John Ek (Pacific Northwest Research Institute) for technical assistance.

REFERENCES

1. Hannun, Y. A., and Bell, R. M. (1989) *Science* **243,** 500–507
2. Merrill, A. H. J., Nimkar, S., Menaldino, D., Hannun, Y. A., Loomis, C. R., Bell, R. M., Tyagi, S. R., Lambeth, J. D., Stevens, V. L., Hunter, R., and Liotta, D. C. (1989) *Biochemistry* **28,** 3138–3145
3. Igarashi, Y., Hakomori, S., Toyokuni, T., Dean, B., Fujita, S., Sugimoto, M., Ogawa, T., El-Ghendy, K., and Racker, E. (1989) *Biochemistry* **28,** 6796–6800
4. Kolesnick, R. N., and Kronke, M. (1998) *Annu. Rev. Physiol.* **60,** 643–665
5. Pettus, B. J., Chalfant, C. E., and Hannun, Y. A. (2002) *Biochim. Biophys. Acta* **1585,** 114–125
6. Kolesnick, R. N. (2002) *J. Clin. Invest.* **110,** 3–8
7. Venkataraman, K., Riebeling, C., Bodennec, J., Riezman, H., Allegood, J. C., Sullards, M. C., Merrill, A. H. J., and Futerman, A. H. (2002) *J. Biol. Chem.* **277,** 35642–35649
8. Smith, W. L., and Merrill, A. H. J. (2002) *J. Biol. Chem.* **277,** 25841–25842
9. Sato, M., Markiewicz, M., Yamanaka, M., Bielawska, A., Mao, C., Obeid, L. M., Hannun, Y. A., and Trojanowska, M. (2003) *J. Biol. Chem.* **278,** 9276–9282
10. Maceyka, M., Payne, S. G., Milstien, S., and Spiegel, S. (2002) *Biochim. Biophys. Acta* **1585,** 193–201
11. Spiegel, S., English, D., and Milstien, S. (2002) *Trends Cell Biol.* **12,** 236–242
12. Payne, S. G., Milstien, S., and Spiegel, S. (2002) *FEBS Lett.* **531,** 54–57
13. Sano, T., Baker, D., Virag, T., Wada, A., Yatomi, Y., Kobayashi, T., Igarashi, Y., and Tigyi, G. (2002) *J. Biol. Chem.* **277,** 21197–21206
14. Kihara, A., Ikeda, M., Kariya, Y., Lee, E.-Y., Lee, Y.-M., and Igarashi, Y. (2003) *J. Biol. Chem.* **278,** 14578–14585
15. Ogawa, C., Kihara, A., Gokoh, M., and Igarashi, Y. (2003) *J. Biol. Chem.* **278,** 1268–1272
16. Megidish, T., Cooper, J., Zhang, L., Fu, H., and Hakomori, S. (1998) *J. Biol. Chem.* **273,** 21834–21845
17. Megidish, T., Takio, K., Titani, K., Iwabuchi, K., Hamaguchi, A., Igarashi, Y., and Hakomori, S. (1999) *Biochemistry* **38,** 3369–3378
18. Fu, H., Subramanian, R. R., and Masters, S. C. (2000) *Annu. Rev. Pharmacol. Toxicol.* **40,** 617–647
19. Megidish, T., Hamaguchi, A., Iwabuchi, K., and Hakomori, S. (2000) *Methods Enzymol.* **312,** 381–387
20. Denning, M. F., Wang, Y., Tibudan, S., Alkan, S., Nickoloff, B. J., and Qin, J.-Z. (2002) *Cell Death Differ.* **9,** 40–52
21. Mineki, R., Taka, H., Fujimura, T., Kikkawa, M., Shindo, N., and Murayama, K. (2002) *Proteomics* **2,** 1672–1681
22. Graves, P. R., and Haystead, T. A. J. (2002) *Microbiol. Mol. Biol. Rev.* **66,** 39–63
23. Zhang, W., and Chait, B. T. (2000) *Anal. Chem.* **72,** 2482–2489
24. Perkins, D. N., Pappin, D. J., Creasy, D. M., and Cottrell, J. S. (1999) *Electrophoresis* **20,** 3551–3567
25. Choudhary, J. S., Blackstock, W. P., Creasy, D. M., and Cottrell, J. S. (2001) *Trends Biotechnol.* **19,** (suppl.) S17–S22
26. Eng, J. K., McCormack, A. L., and Yates, J. R. (1994) *J. Am. Soc. Mass Spectrom.* **5,** 976–989
27. Hancock, W. S., Wu, S.-L., and Shieh, P. (2002) *Proteomics* **2,** 352–359
28. Ono, Y., Fujii, T., Ogita, K., Kikkawa, U., Igarashi, K., and Nishizuka, Y. (1988) *J. Biol. Chem.* **263,** 6927–6932
29. Megidish, T., White, T., Takio, K., Titani, K., Igarashi, Y., and Hakomori, S. (1995) *Biochem. Biophys. Res. Commun.* **216,** 739–747
30. Grant, S., and Spiegel, S. (2002) *J. Clin. Invest.* **109,** 717–719
31. Spiegel, S., and Milstien, S. (1995) *J. Membr. Biol.* **146,** 225–237
32. Coroneos, E., Martinez, M., McKenna, S., and Kester, M. (1995) *J. Biol. Chem.* **270,** 23305–23309
33. Snell, E. E., Dimari, S. J., and Brady, R. N. (1970) *Chem. Phys. Lipids* **5,** 116–138
34. Ohta, H., Sweeney, E. A., Masamune, A., Yatomi, Y., Hakomori, S., and Igarashi, Y. (1995) *Cancer Res.* **55,** 691–697
35. Igarashi, Y., and Hakomori, S. (1989) *Biochem. Biophys. Res. Commun.* **164,** 1411–1416
36. Mano, N., Oda, Y., Yamada, K., Asakawa, N., and Katayama, K. (1997) *Anal. Biochem.* **244,** 291–300
37. Edsall, L. C., Van Brocklyn, J. R., Cuvillier, O., Kleuser, B., and Spiegel, S. (1998) *Biochemistry* **37,** 12892–12898
38. Li, S., Janosch, P., Tanji, M., Rosenfeld, G. C., Waymire, J. C., Mischak, H., Kolch, W., and Sedivy, J. M. (1995) *EMBO J.* **14,** 685–696
39. Roy, S., McPherson, R. A., Apolloni, A., Yan, J., Lane, A., Clyde-Smith, J., and Hancock, J. F. (1998) *Mol. Cell Biol.* **18,** 3947–3955
40. Zha, J., Harada, H., Yang, E., Jockel, J., and Korsmeyer, S. J. (1996) *Cell* **87,** 619–628
41. Yang, H., Masters, S. C., Wang, H., and Fu, H. (2001) *Biochim. Biophys. Acta* **1547,** 313–319
42. Datta, R., Banach, D., Kojima, H., Talanian, R. V., Alnemri, E. S., Wong, W. W., and Kufe, D. W. (1996) *Blood* **88,** 1936–1943
43. Ghayur, T., Hugunin, M., Talanian, R. V., Ratnofsky, S., Quinlan, C., Emoto, Y., Pandey, P., Datta, R., Huang, Y., Kharbanda, S., Allen, H., Kamen, R., Wong, W., and Kufe, D. (1996) *J. Exp. Med.* **184,** 2399–2404
44. Koriyama, H., Kouchi, Z., Umeda, T., Saido, T. C., Momoi, T., Ishiura, S., and Suzuki, K. (1999) *Cell. Signal.* **11,** 831–838
45. Basu, A., Woolard, M. D., and Johnson, C. L. (2001) *Cell Death Differ.* **8,** 899–908
46. Brodie, C., and Blumberg, P. M. (2003) *Apoptosis* **8,** 19–27
47. Muslin, A. J., Tanner, J. W., Allen, P. M., and Shaw, A. S. (1996) *Cell* **84,** 889–897
48. Yaffe, M. B., Rittinger, K., Volinia, S., Caron, P. R., Aitken, A., Leffers, H., Gamblin, S. J., Smerdon, S. J., and Cantley, L. C. (1997) *Cell* **91,** 961–971

Available online at www.sciencedirect.com
SCIENCE DIRECT®
Molecular & Biochemical Parasitology 128 (2003) 175–186
MOLECULAR & BIOCHEMICAL PARASITOLOGY

Isolation and characterization of the stage-specific cytochrome *b* small subunit (CybS) of *Ascaris suum* complex II from the aerobic respiratory chain of larval mitochondria

Hisako Amino[a], Arihiro Osanai[a], Hiroko Miyadera[a], Noriko Shinjyo[a], Eriko Tomitsuka[a], Hikari Taka[b], Reiko Mineki[b], Kimie Murayama[b], Shinzaburo Takamiya[c], Takashi Aoki[c], Hideto Miyoshi[d], Kimitoshi Sakamoto[d], Somei Kojima[e], Kiyoshi Kita[a,*]

[a] *Department of Biomedical Chemistry, Graduate School of Medicine, The University of Tokyo, Tokyo, Japan*
[b] *Division of Biochemical Analysis, Central Laboratory of Medical Sciences, School of Medicine, Juntendo University, Tokyo, Japan*
[c] *Department of Parasitology, School of Medicine, Juntendo University, Tokyo, Japan*
[d] *Division of Applied Life Sciences, Graduate School of Agriculture, Kyoto University, Kyoto, Japan*
[e] *Department of Parasitology, The Institute of Medical Science, The University of Tokyo, Tokyo, Japan*

Received 10 December 2002; received in revised form 11 March 2003; accepted 11 March 2003

Abstract

We recently reported that *Ascaris suum* mitochondria express stage-specific isoforms of complex II: the flavoprotein subunit and the small subunit of cytochrome *b* (CybS) of the larval complex II differ from those of adult enzyme, while two complex IIs share a common iron–sulfur cluster subunit (Ip). In the present study, *A. suum* larval complex II was highly purified to characterize the larval cytochrome *b* subunits in more detail. Peptide mass fingerprinting and N-terminal amino acid sequencing showed that the larval and adult cytochrome *b* (CybL) proteins are identical. In contrast, cDNA sequences revealed that the small subunit of larval cytochrome *b* ($CybS^L$) is distinct from the adult CybS ($CybS^A$). Furthermore, Northern analysis and immunoblotting showed stage-specific expression of $CybS^L$ and $CybS^A$ in larval and adult mitochondria, respectively. Enzymatic assays revealed that the ratio of rhodoquinol-fumarate reductase (RQFR) to succinate-ubiquinone reductase (SQR) activities and the K_m values for quinones are almost identical for the adult and larval complex IIs, but that the fumarate reductase (FRD) activity is higher for the adult form than for the larval form. These results indicate that the adult and larval *A. suum* complex IIs have different properties than the complex II of the mammalian host and that the larval complex II is able to function as a RQFR. Such RQFR activity of the larval complex II would be essential for rapid adaptation to the dramatic change of oxygen availability during infection of the host.

Keywords: *Ascaris suum*; Succinate dehydrogenase; Fumarate reductase; Large subunit of cytochrome *b*; Small subunit of cytochrome *b*

1. Introduction

The mitochondrial respiratory chain of the parasitic nematode, *Ascaris suum*, changes dramatically during its life cycle [1–7]. *A. suum* larvae in the free-living stage inhabit the air (~160 mmHg), whose mitochondria utilize classic mammalian-type aerobic respiration [1,2]. In contrast, the mitochondria of the adult worm utilize an anaerobic NADH-fumarate reductase system as a major component of the respiratory chain [2]. This switch allows respiration by the adult worm in the host small intestine where there is limited oxygen tension (0–10 mmHg) [2]. Quinones, low molecular weight electron carriers that transfer electrons between respiratory complexes, also change markedly during the *A. suum* life cycle. The larvae employ ubiquinone

Abbreviations: Fp, flavoprotein; Ip, iron–sulfur cluster subunit; L3, third stage larva; CybL, large subunit of cytochrome *b*; CybS, small subunit of cytochrome *b*; Fp^L, larval Fp, Fp^A; adult Fp; $CybS^L$, larval CybS, $CybS^A$; adult CybS; PCR, polymerase chain reaction; RT-PCR, reverse transcription PCR; SDH, succinate dehydrogenase; FRD, fumarate reductase; SQR, succinate-ubiquinone reductase; QFR, quinol-fumarate reductase; RQFR, rhodoquinol-fumarate reductase; SL, spliced leader; RACE, rapid amplification of cDNA ends; Dig, Digoxigenin; NJ, neighbor joining; ML, maximum likelihood; SH, Shimodaira–Hasegawa; PGL, paraganglioma; PAGE, polyacrylamide gel electrophoresis; SDS, sodium dodecyl sulfate; CBB, Coomassie brilliant blue; HPLC, high performance liquid chromatography

* Corresponding author. Tel.: +81-3-5841-3526; fax: +81-3-5841-3444.
E-mail address: kitak@m.u-tokyo.ac.jp (K. Kita).

0166-6851/03/$ – see front matter © 2003 Elsevier Science B.V. All rights reserved.
doi:10.1016/S0166-6851(03)00074-4

and electron transport functions as it does in mammals. In contrast, in the adult *A. suum*, the major quinone is the low-potential quinone, rhodoquinone, an essential component of the NADH-fumarate reductase system.

In the aerobic energy metabolism, complex II is involved both in the tricarboxylic acid (TCA) cycle and the electron transport chain: it catalyzes the oxidation of succinate to fumarate and transfers the reducing equivalent to ubiquinone (succinate-ubiquinone reductase; SQR). In the anaerobic electron transfer system, complex II carries out fumarate reduction using quinol as an electron donor (quinol-fumarate reductase; QFR), in other words, the reverse reaction of SQR.

Complex II is generally composed of four polypeptides [8]. The largest, the flavoprotein (Fp; SDHA) subunit, has an apparent molecular mass of approximately 70 kDa and contains covalently bound flavin. The second largest subunit, the iron–sulfur protein (Ip; SDHB), has an apparent molecular mass of approximately 30 kDa and contains iron–sulfur clusters: [2Fe–2S], [4Fe–4S] and [3Fe–4S]. The Fp and Ip subunits form the catalytic portion of complex II and appear to be highly conserved. This portion acts as a succinate dehydrogenase (SDH), catalyzing the oxidation of succinate by water-soluble electron acceptors such as phenazine methosulfate (PMS) in SQR, while it acts as a fumarate reductase (FRD), catalyzing electron transfer from water-soluble electron donors such as reduced methylviologen (MV) to fumarate in QFR. Cytochrome *b* is composed of the two remaining subunits, the 15 kDa CybL (SDHC, QPs1 or C_{II-3}) and the 13 kDa CybS (SDHD, QPs3 or C_{II-4}). These two proteins possess hydrophobic membrane anchors. They act together to ligate heme *b*, and they appear to be essential for the interaction between complex II and the quinone, although there is little conservation in their amino acid sequences between species.

Complex II from the adult *A. suum* mitochondria exhibits high FRD activity and functions as a terminal oxidase in the NADH-fumarate oxidoreductase system of anaerobic metabolism. In contrast, complex II from free-living third stage larvae (L3; [9]) shows lower FRD activity and functions as a SDH during aerobic respiration [10–12]. Thus, complex II plays a key role in the two different energy metabolism systems of *A. suum* [13]. To elucidate the molecular mechanism of the transition from aerobic to anaerobic metabolism, we have been studying the stage-specific isoforms of *A. suum* complex II.

Our previous biochemical analyses showed that at least the Fp and CybS subunits are different between the adult and larval forms of complex II [13]. Amino acid sequences of two stage-specific Fp deduced from cDNA showed 79% homology [2,14,15]. In addition, by the protein chemical analysis, we found that the stage-specific forms of *A. suum* complex II share a common Ip although they possess distinct enzymatic properties [16]. Furthermore, cytochrome b_{558} of *A. suum* adult complex II is reducible by succinate [10], and has an Em' of −34 mV [17], which is higher than that of the cytochrome b_{560} in bovine heart complex II (−185 mV) [18]. This relatively positive Em' of the cytochrome b_{558} may facilitate electron transfer from reduced rhodoquinone (rhodoquinol, −63 mV) to succinate/fumarate couple (+30 mV), although the participation of heme *b* in electron transfer by complex II is not proven. In addition, the Soret band of the oxidized larval form (402 nm) of cytochrome *b* is different from that of the adult enzyme (410 nm) [13]. The Em' of the cytochrome *b* in larval complex II seems to be lower than that of adult, because cytochrome *b* of complex II is not detectable in the larval mitochondria after succinate reduction [1]. Further, the larval cytochrome *b* utilizes ubiquinone, a high potential quinone (+110 mV) [1], as the electron acceptor. Collectively, these results strongly suggest that the larval and adult complex IIs possess different forms of cytochrome *b*.

Determination and comparison of the primary structure of the adult and larval *A. suum* complex IIs can help clarify and understand their unique properties. The structural similarity and evolutionary conservation of the amino acid sequences of the Fp and Ip subunits have facilitated the cloning of these cDNAs by homology probing with degenerate primers in a polymerase chain reaction (PCR) [2,14–16,19]. We cloned two cDNAs for Fp's from the larval and adult enzymes [2,14,15] and found that complex IIs share a common Ip [16,19]. The same strategy was used for cloning the cDNA for the adult CybL [5], while the cDNA for the adult CybS ($CybS^A$) was isolated from an adult muscle cDNA library using a monoclonal antibody against $CybS^A$ [20]. However, we were unable to obtain cDNA sequences of the larval cytochrome *b* because of the low conservation of amino acid sequences [20] and the lack of an antibody to $CybS^L$.

In the present study, *A. suum* larval complex II was highly purified so that we could identify the larval cytochrome *b* subunits and study the enzymatic properties of the larval complex II. Biochemical and Northern analyses of the larval CybL and its mRNA showed that it is identical to the adult CybL. In addition, we obtained cDNA for $CybS^L$, which revealed that the larval protein is more closely related to CybS of the free-living nematode *Caenorhabditis elegans* than to *A. suum* $CybS^A$. Kinetic analyses of the purified complex IIs showed that larval complex II is also able to catalyze rhodoquinol-fumarate reductase (RQFR), even though its FRD is lower than adult complex II.

2. Materials and methods

2.1. Culture of A. suum larvae and the isolation of mitochondria from A. suum

Fertilized eggs, L3 and L3 mitochondria were prepared as previously described [1]. Mitochondria from adult *A. suum* muscle were isolated as described except that Nagase pretreatment was omitted [10].

2.2. Preparation of A. suum larval complex II

Purification of complex II from *A. suum* larval mitochondria was basically performed as described previously [16]. For separation by ion exchange column chromatography, mitochondria (32 mg) were treated with a nonionic detergent, sucrose monolaurate (2.5%, w/v), in 10 mM Tris–HCl (pH 7.5). After centrifugation at 200,000 × *g* for 60 min, the supernatant was applied to a DEAE-Cellulofine A-500 column (1.2 cm × 4.4 cm) equilibrated with 0.1% (w/v) sucrose monolaurate in 10 mM Tris–HCl (pH 7.5). Complex II was eluted with the same buffer containing a 100 ml linear gradient of 0–0.15 M NaCl at a flow rate of 30 ml h^{-1}. Highly purified larval complex II was obtained by re-chromatography under the same conditions used for the first column. The adult complex II was also purified by this protocol.

2.3. N-terminal amino acid sequence analysis

The larval complex II (approximately 5 μg) was separated using sodium dodecyl sulfate–polyacrylamide gel electrophoresis (SDS–PAGE) with a 10–20% gradient gel (Biocraft, Japan) as described in the previous report [16]. The gel was transblotted onto a polyvynilidene difluoride (PVDF) membrane (Immobilon-PSQ, Millipore Co., USA) using the tank blotting method and 10 mM 3-(cyclohexylamino)-1-propanesulfonic acid in 10% methanol, pH 11, 50 V for 45 min [21]. The proteins on the electroblotted membrane were stained with 0.1% Coomassie brilliant blue (CBB) R-350 (Amersham Pharmacia Biotech, Sweden). The protein bands at 15 and 13 kDa (CybL and CybS) from larval complex II were subjected to N-terminal sequencing with an automated protein sequencer (Hewlett Packard G1005A, USA).

2.4. In-gel digestion, mass spectrometry and sequencing

The CybL subunits separated by SDS–PAGE were identified by peptide mass fingerprinting and sequencing (APRO Life Science Institute, Inc., Japan). The adult and larval complex IIs were alkylated by acrylamide and subjected to SDS–PAGE. The bands of the CybL protein were excised from gel, and cleaved in-gel with trypsin [22]. In brief, the gel pieces were dried after washing twice, and then soaked in Tris buffer (pH 8.0) containing trypsin at 35 °C for 20 h. The peptide mixtures were trapped on ZipTip C18 (Millipore Co., USA), eluted in 1 μl of 70% acetonitrile, 1% formic acid, and analyzed by nanoflow electrospray ionization mass spectrometry (ESI-MS) for peptide mass fingerprinting using Q-Tof2 system (Micromass UK, UK) [23]. The mass spectra containing fragment ions in multiple charge states were replotted onto a single spectrum of monovalent ions using MaxEnt3 software. The amino acid sequences of several tryptic peptides from the larval CybL protein were determined by APRO Life Science Institute, Inc. The in-gel-digested tryptic peptides were eluted from gel, and then separated on TSKgel ODS-80Ts QA (2.0 mm × 250 mm, TOSOH, Japan). N-terminal sequence analysis was performed using a Procise 494 Protein Sequencing System.

2.5. Isolation of RNA and RT-PCR

Poly(A)+RNAs were prepared as previously reported [16]. *A. suum* muscle was isolated from adult female worms within 3 h of collection. *A. suum* L3, prepared as described previously [1], was stored at −80 °C until use. Total RNA from the adult muscle and L3 worms were extracted according to Chomczynski and Sacchi [24]. For Northern hybridization, poly(A)+RNA from adult was purified on an Oligo (dT)-Cellulose column (Pharmacia), and poly(A)+RNA from L3 was isolated using Oligotex-dT30 (Takara, Japan). For cloning of cDNA for the larval CybS subunit, poly(A)+RNA was isolated from the L3 total RNA using an Oligo (dT)-Cellulose column (Pharmacia Biotech, Sweden).

cDNAs were synthesized from about 2 μg of mRNA and random primer $(N)_6$ (Takara, Japan) using a Mo-MuLV reverse transcriptase (GIBCOBRL, Life Technologies, USA). The PCR reaction was performed using a *Taq* DNA polymerase (GIBCOBRL, Life Technologies, USA) or *Ex-Taq* DNA polymerase (Takara, Japan) according to each manufacturer's instructions. The PCR programs were carried out as described in each section.

2.6. Isolation of cDNA encoding the CybS subunit of larval complex II

Cloning of the cDNA fragment for the N-terminal amino acid sequence of the larval CybS was carried out by nested PCR. RT-PCR was performed using a forward primer p-80 designed based on the spliced leader sequence 1 (SL1) of the nematode, 5′-GGTTTAATTACCCAAGTTTGAG-3′ [25], and a reverse primer p-355, 5′-ATCATNCCNGCNGC(A/G)TA-3′ based on the amino acid sequence YAAGMI (residues 26–31 obtained from the N-terminal amino acid sequence), and subjected to 30 cycles of the following conditions: 95 °C for 30 s, 50 °C for 30 s and 72 °C for 1 min. The product of the first reaction was used as a template for a second reaction with the two nested primers p-353 (a forward primer), 5′-GTNACNACNCCNGTN(A/T)(C/G)N(C/A)G-3′ based on the sequence VTTPVSR (residues 2–8 from the N-terminal sequence analysis), and p-356 (a reverse primer), 5′-(A/G)TGNA(A/G)N(G/C)(A/T)(A/G)TG(A/G)TC(T/C)-TC(A/G/T)AT-3′ based on the sequence IEDHSLH (residues 13–19 from the N-terminal sequence analysis). PCR was carried out for 30 cycles under the following conditions: 95 °C for 30 s, 42 °C for 30 s, 72 °C for 1 min. This resulted in a product with the expected size (54 bp). Next, 5′ rapid amplification of cDNA ends (RACE) was performed using SL1 primer p-80 and P-378, 5′-TCTTCTATCGAAAAA-GGTTCCC-3′ based on the above product, followed by

cloning and sequencing. For 3′ RACE, PCR was carried out using P-386 (AARTSVTT obtained from 5′ RACE) 5′-AGCGCGGACGAGTGTCACTAC-3′ and P-384 (adaptor-1) 5′-TGGAAGAATTCGCGGCCGCAG-3′ as primers and cDNA synthesized from the larval poly(A)+ RNA and P-383 5′-AACTGGAAGAATTCGCGGCCGCA-GGAATTTTTTTTTTTTTTTTTT-3′ as a template. Nested PCR was then carried out using P-377 (REPFSI obtained from 5′ RACE) 5′-GGGAACCTTTTTCGATAGA-3′ and P-385 (adaptor-2) 5′-GAATTCGCGGCCGCAG-3′ as primers and the first PCR product as a template. The PCR products were cloned into a plasmid vector using a TA cloning kit (Invitrogen). Japan Bio Servis, Japan, synthesized all oligonucleotides used as primers for PCR.

2.7. DNA sequencing

The nucleotide sequences were obtained using a dye primer system (Thermo Sequenase fluorescent-labeled primer cycle sequencing Kit with 7-deaza-dGTP, Amersham Pharmacia Biotech, UK) using a DNA sequencer DSQ-2000L (Shimadzu, Japan). Sequences were analyzed with GENETYX ver.9 and ATSQ ver.3.0 software packages. The nucleotide sequence data of $CybS^{L}$ reported in this paper is available in the DDBJ, EMBL and GenBank databases under the accession number AB071995.

2.8. Phylogenetic analysis

Phylogenetic reconstruction analysis for amino acid sequences of CybS was performed by the neighbor joining (NJ) method in Clustal X version 1.81 program [26]. Distance matrix was estimated by the NJ method in Clustal X version 1.81 program [26]. In order to compare alternative trees of interest, the maximum likelihood (ML) method with a rate-across-site model was used by the CODEML program in the PAML package [27]. The JTT-F+ gamma model was assumed for the amino acid substitution process [27]. Log-likelihoods of alternative trees were compared by Shimodaira–Hasegawa (SH) test in the CONSEL program [28].

2.9. Northern hybridization

RNA electrophoresis was performed using a standard formaldehyde gel [29]. Northern hybridization was carried out using high SDS concentration buffer according to the recommended protocol (Boehringer Manheim) except that 50% formamide was omitted as described previously [16]. Digoxigenin (Dig)-labeled nucleotides for Northern hybridization were prepared using hexanucleotides, Klenow enzyme (Boehringer Manheim) and the coding sequence of each cDNA as a template: bases 32–598 of accession number D78157 for the CybL, bases 23–493 of accession number D78158 for the $CybS^{A}$ and bases 68–493 of accession number AB071995 for the $CybS^{L}$ cDNA. Dig-labeled nucleotides were detected by a chemiluminescent reaction using disodium 3-(4-methoxyspiro{1,2-dioxetane-3,2′-(5′-chloro)tricyclo[3.3.1.1]decan}-4-yl) phenyl phosphate (Boehringer Manheim) as a substrate.

2.10. Preparation of a peptide-based antibody to the larval CybS subunit

Two synthetic peptides containing a cysteine at each C-terminus: (NH_2-SVTTPVSREPFSIE-COOH, amino acids 1–14) corresponding to the $CybS^{L}$-specific N-terminal region, and (NH_2-KIKNEVDPTLTFRRSC-COOH, amino acids 74–89) located in the preceding S-1 region of Ip were synthesized by Peptide Institute Inc., Japan. The peptides were conjugated to keyhole limpet haemocyanin and injected along with an adjuvant into rabbits. The peptide-based antibody to the $CybS^{L}$ was purified from anti-sera by affinity column chromatography using a bound peptide, and elution with $MgCl_2$. The peptide-based antibody to the Ip was purified in the same manner except the antibody was eluted with KSCN.

2.11. Enzymatic activities

SQR, RQFR and FRD were assayed as described in previous reports [16,30,31].

2.12. Other methods

Spectrophotometric measurements were performed at room temperature with a Shimadzu UV-3000 dual wavelength spectrophotometer. Protein was determined according to Lowry et al. [32] with bovine serum albumin as a standard. Western blotting was performed according to Towbin et al. [33] using an alkaline phosphatase system for detection.

3. Results

3.1. Identification of the anchor subunits of A. suum larval complex II

Studies of complex II using preparations of larval and adult mitochondria are complex and difficult to interpret. Therefore, analysis of purified larval complex II is essential to understand the differences between the anchor subunits of larval and adult complex IIs and to clarify their physiological roles in the *A. suum* life cycle. Purification of the larval complex II has been difficult because only small amount of mitochondria can be obtained from L3. For this reason, we established a small-scale protocol to purify larval complex II (see Section 2). We obtained a highly purified larval complex II from larval mitochondria by extraction with sucrose

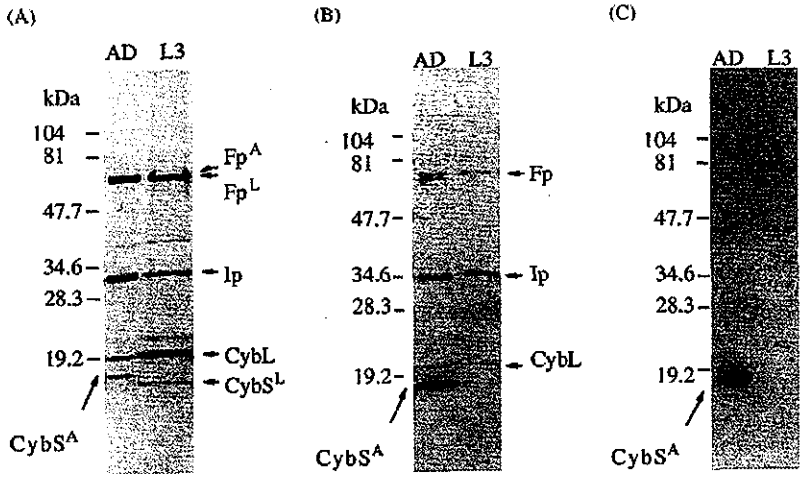

Fig. 1. (A) CBB-stained SDS–PAGE gel of larval complex II. Immunoblotting of complex II with (B) antibodies against all the subunits of *A. suum* adult complex II or (C) with a monoclonal antibody against $CybS^A$ that recognizes the peptide VNDYGRPF (residues 79–86 of the mature form of $CybS^A$) which is located in the loop connecting transmembrane helix 2 with 3 (lower case letters in Fig. 7A). Larval complex II was purified from larval mitochondria as described in Section 2. AD, complex II purified from *A. suum* adult; L3, complex II from *A. suum* third stage larvae mitochondria.

monolaurate, followed by DEAE-Cellulofine column chromatography. At least 30 mg of larval mitochondria was required to obtain reproducible results. This protocol was also useful for the purification of adult complex II. The preparations of larval and adult complex IIs were more than 90% pure (Fig. 1). Two bands with small molecular masses in larval complex II were likely the larval forms of CybL and CybS because their staining intensities were stoichiometric with the other subunits. Polyclonal antibodies against each of the adult complex II subunits recognized all of the subunits of the purified larval complex II except CybS (Fig. 1B). A monoclonal antibody against $CybS^A$ also did not react with the smallest band in purified larval complex II (Fig. 1C). These results are consistent with previous observations in the larval and adult mitochondria [13].

A band with same molecular mass as adult CybL has not been identified in previous Western blots of larval mitochondria. This could be due to a low titer of antibody against adult CybL. Indeed, our results showing cross-reactivity between larval and adult CybL suggested that the larval and adult complex IIs of *A. suum* share not only a common Ip but also a common CybL. To examine this possibility further, we analyzed the primary structure of the CybL in the larval complex II. The larval CybL was separated by SDS–PAGE (Fig. 1A), transferred to a PVDF membrane, and the N-terminal amino acid sequence was determined. We found that the N-terminal 30 amino acid sequence of larval CybL was identical to that of the adult CybL. We further examined the internal amino acid sequences of the adult and larval forms of CybL from tryptic peptides. The N-terminal sequences of four fragments (shown in boldface in Fig. 2) were separated by HPLC. These were also identical to the corresponding sequences of adult CybL. In addition, the molecular masses of tryptic peptides, T1–2, T5, T7, T8, T9, T10 and T11–12, obtained by nano ESI-MS were very close to their predicted values, although several theoretical fragments were not obtained (Table 1 and amino acids underlined in Fig. 2). These results, together with the size and antigenic properties of the CybL proteins, strongly suggest that the larval and adult forms of this protein are identical.

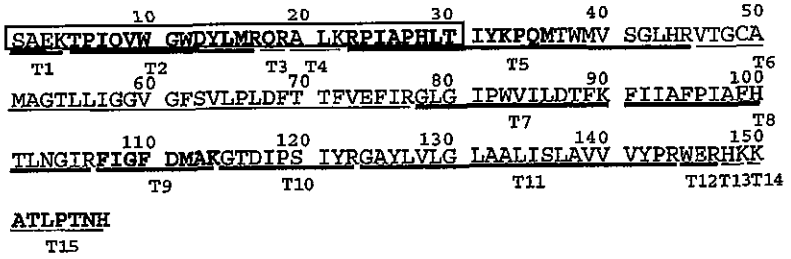

Fig. 2. Amino acid sequence of CybL. The 30 amino acid sequence determined by N-terminal sequencing is marked with an open box. The T1–15 fragments indicate the theoretical tryptic peptides from the *A. suum* CybL. Boldface letters represent the tryptic peptides detected by Edman degradation. The T1–2, T5, T7–12 fragments detected by the peptide mass fingerprinting are thick underlined.

Table 1
Peptide mass fingerprinting of tryptic peptides from the adult and larval CybL

Peptide	Residues (amino acids)	Theoretical value (*m/z*)	Charge of ion	Adult (*m/z*)	L3 (*m/z*)	Sequence
T1	1–4			N.D.	N.D.	SAEK
T2	5–17	840.91	2+	840.9077	840.9702	TPIQVWGWDYLMR
T1–2	1–17	699.35	3+	N.D.	699.3978	SAEKTPIQVWGWDYLMR
T3	18–19			N.D.	N.D.	QR
T4	20–22			N.D.	N.D.	ALK
T5	23–45	553.70	5+	553.6808	553.7224	RPIAPHLTIYKPQMTWMVSGLHR
T6	46–77			N.D.	N.D.	VTGCAMAGTLLIGGVGFSVLPLDFTTFVEFIR
T7	78–90	729.92	2+	729.9075	729.9578	GLGIPWVILDTFK
T8	91–106	915.53	2+	915.5168	915.5175	FIIAFPIAFHTLNGIR
		610.69	3+	610.6752	610.7206	
T9	107–114	472.73	2+	472.7208	472.7742	FIGFDMAK
T8–9	91–114	919.17	3+	N.D.	919.1786	FIIAFPIAFHTLNGIRFIGFDMAK
		689.63	4+	N.D.	N.D.	
T10	115–123	511.27	2+	511.2812	511.3128	GTDIPSIYR
T11	124–144			N.D.	N.D.	GAYLVLGLAALISLAVVVYPR
T12	145–147			N.D.	N.D.	WER
T11–12	124–147	877.18	3+	N.D.	877.1080	GAYLVLGLAALISLAVVVYPRWER
T13	148–149			N.D.	N.D.	HK
T14	150–150			N.D.	N.D.	K
T15	151–157			N.D.	N.D.	ATLPTNH

3.2. Molecular cloning of cDNA for the larval CybS ($CybS^L$) subunit

In contrast to CybL, protein chemical and immunochemical analyses suggested that $CybS^L$ is distinct from $CybS^A$. In fact, homology probing by degenerated primers failed because of low conservation of amino acid sequence. We observed an approximately 14 kDa peptide in the larval complex II that was likely $CybS^L$ because its N-terminal sequence was related to that of $CybS^A$ and CybS of *C. elegans* [20,34]. We attempted to use this information to clone the cDNA for $CybS^L$. First, mixed primers were designed from the N-terminal amino acid sequence of $CybS^L$. A PCR product with the expected size (54 bp) was obtained by RT-PCR of the larval poly(A)+RNA. This sequence was identical to the corresponding N-terminal amino acid sequence except for Trp-26, which was taken for tyrosine in the sequencing by Edman degradation because of the acid-lability of tryptophan. To obtain the full-length cDNA, we performed the RACE (see Section 2). We obtained a cDNA sequence of the *A. suum* $CybS^L$ containing the SL sequence and an open reading frame of 423 nucleotides encoding a protein of 141 amino acids. This protein contains a 24 amino acid putative mitochondrial presequence that is rich in basic amino acids, such as arginine, and the hydroxylated amino acids serine and threonine. This is a characteristic of the cleavable N-terminal presequences that are essential for the import of mitochondrial proteins encoded by nuclear DNA [35]. Thus, the mature larval CybS contains 117 amino acids with a calculated molecular mass of 12,948 Da. This value is slightly smaller than that estimated by SDS–PAGE (14.2 kDa in Fig. 1A). This is not surprising, as many membrane proteins migrate anomalously on SDS–PAGE [36].

A comparison of the amino acid sequence of the *A. suum* $CybS^L$ with *A. suum* adult [20], *C. elegans* [34], human [37], bovine [38] and *Saccharomyces cerevisiae* [39] CybS is shown in Fig. 3. The deduced amino acid sequence contains a conserved histidine residue (His-80, closed arrowhead in Fig. 3) in the second transmembrane region that is a putative binding site for the heme *b* molecule [38,40,41]. The degree of amino acid identity between the *A. suum* $CybS^L$ and the free-living nematode *C. elegans* CybS (59%) was higher than that between the *A. suum* $CybS^L$ and the *A. suum* $CybS^A$ (56%). The phylogenetic tree using the NJ method also showed with 80% bootstrap support that $CybS^L$ is more closely related to the CybS of *C. elegans* than to $CybS^A$ (Fig. 4). In order to compare alternative trees possible for the relationships among three genes from $CybS^L$, $CybS^A$ and *C. elegans* CybS, the ML analysis with a rate-across-site model was examined for three possible trees. The best tree was same as the one shown in Fig. 4 (data not shown). The log-likelihood differences between the best tree and the alternative tree in which the two *A. suum* genes share a most recent common ancestor, and the one in which the *A. suum* adult and the *C. elegans* genes share a most recent common ancestor, were 0.4 and 0.7, respectively. The SH test showed that the differences are not statistically significant ($P > 0.05$).

3.3. Stage-specific expression of the cytochrome b subunits

In addition to examining the biochemical properties of the cytochrome *b* subunit proteins from the two stage-specific

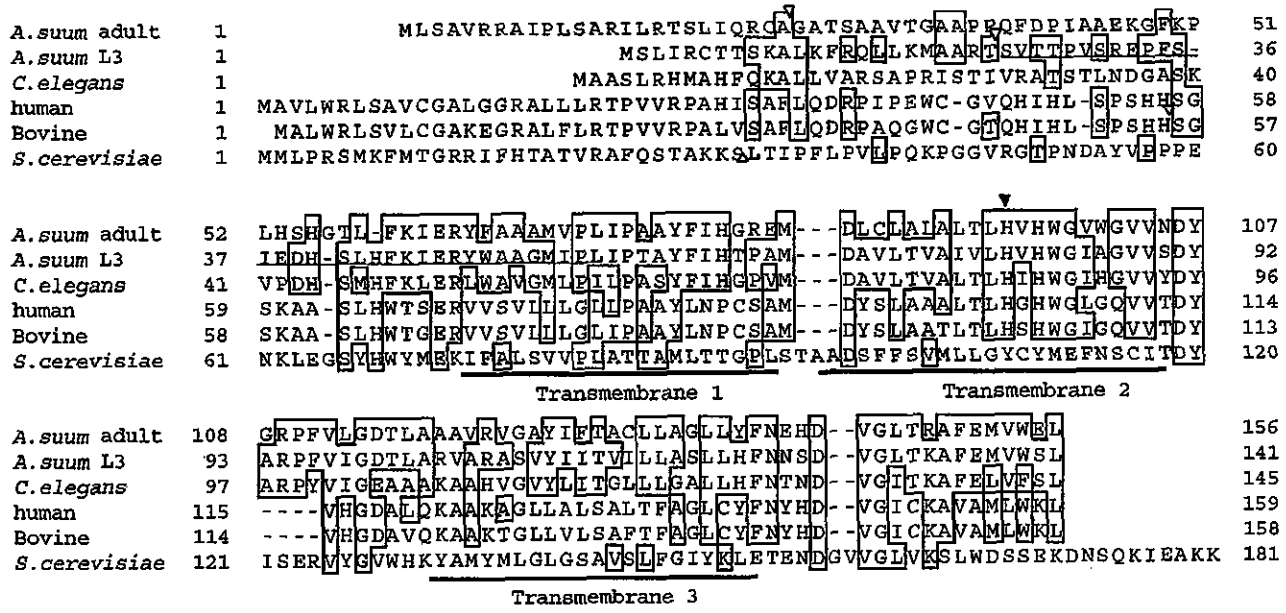

Fig. 3. Comparison of the amino acid sequences of the CybS subunits from various species. The references and accession numbers for each sequence are as follows: *A. suum* adult [20] (P92507); *A. suum* L3 (AB072354); *C. elegans* [34] (O62215); human [37] (O14521); bovine [38] (ABB09426); *S. cerevisiae* [39] (AAA19637). Numbers indicate the positions of amino acids from the first methionine in the CybS subunit from each organism. The partial amino acid sequence of *A. suum* L3 CybS determined from N-terminal sequencing is underlined. Identical amino acids are boxed. The open arrowheads indicate the N-terminal sequence of the *A. suum* adult, L3, bovine and *S. cerevisiae* peptides. The closed arrowhead indicates a putative binding site for heme *b* molecule.

complex IIs, we examined their expression by Northern blotting. Using the cDNA for CybL as a probe, a 0.91 kb poly(A)+RNA was detected in L3 as well as adult *A. suum* muscle (Fig. 5A). This is consistent with the finding that CybL was a common subunit in adult and larval complex IIs. In contrast to CybL, the 0.71 kb transcript of $CybS^{A}$ and the 0.83 kb band of $CybS^{L}$ were exclusively found in the transcripts of adults and L3, respectively (Fig. 5B and C). Stage-specific expression of $CybS^{L}$ in the L3 mitochondria was also shown by Western blotting with an antibody specific to the N-terminus of $CybS^{L}$ (Fig. 6). These results indicate that expression of the two distinct CybS subunits is controlled by a stage-specific transcriptional system.

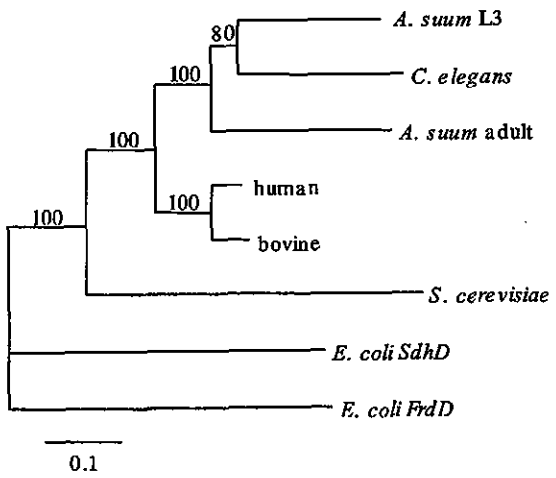

Fig. 4. Phylogenetic tree based on the deduced amino acid sequences of various CybS proteins. The tree was constructed by the NJ method in Clustal X version 1.81 program [26]. The horizontal length indicates the estimated number of substitutions per site. Bootstrap probabilities were calculated with 1000 samplings. *Escherichia coli sdhD* [51] and *Escherichia coli frdD* [52] are presented, and other sequences are already described in Fig. 3.

3.4. Kinetic properties of the larval A. suum complex II

We compared the FRD, RQFR and SQR activities of the larval, adult and bovine heart complex IIs to further understand their functional differences. As is shown in Table 2, bovine heart complex II had a lower ratio of RQFR to SQR and a reduced affinity for fumarate compared to larval and adult *A. suum* complex IIs. The K_m values for *n*-decyl-rhodoquinol (RQH_2) in RQFR and *n*-decyl-ubiquinone (DB) in SQR were nearly the same for the larval and adult enzymes. Interestingly, the ratios of the V_{max}(RQFR) to V_{max}(SQR) were similar for the larval and adult complex IIs, even though the ratio of FRD to SQR for the larval complex II was 19-fold lower than for the adult enzyme. These results indicated that the properties of the two stage-specific *A. suum* complex IIs are substantially different than for the complex II of the mammalian host. In addition, the results show that the larval complex

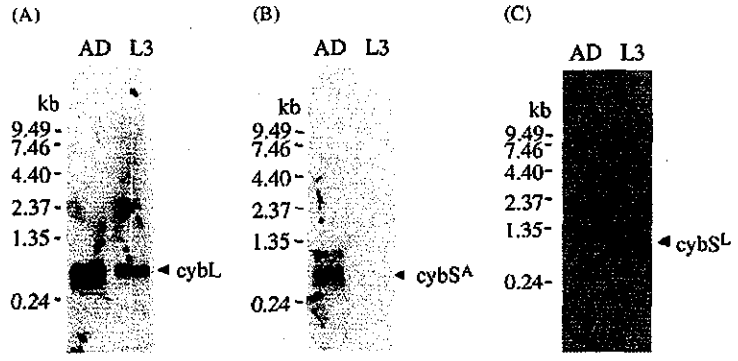

Fig. 5. Northern blotting using (A) adult CybL cDNA, (B) adult CybS cDNA, and (C) larval CybS as probes. AD, adult poly(A)+RNA (1.25 μg); L3, *A. suum* larval poly(A)+RNA (1.28 μg). The size marker is RNA ladder (GIBCOBRL, Life Technologies, USA).

Table 2
Properties of larval and adult complex IIs purified from *A. suum* mitochondria

Enzyme	FRD	RQFR			SQR			FRD/SQR	RQFR/SQR
		V_{max}[a]	K_m[b]		V_{max}[a]	K_m[b]			
			Fumarate	RQH_2[c]		Succinate	DB[d]		
Larval complex II	2.95	2.99	28.5	47.3	7.53	385	12.0	0.39	0.40
Adult complex II	10.46	0.89	16.6	40.6	1.39	625	11.4	7.53	0.64
Bovine complex II	N.D.[e]	0.061	111	74.0	2.19	909	14.0	N.D.[e]	0.028

[a] μmol min^{-1} mg^{-1}.
[b] μM.
[c] *n*-Decyl-rhodoquinol.
[d] *n*-Decyl-ubiquinone.
[e] Not detected.

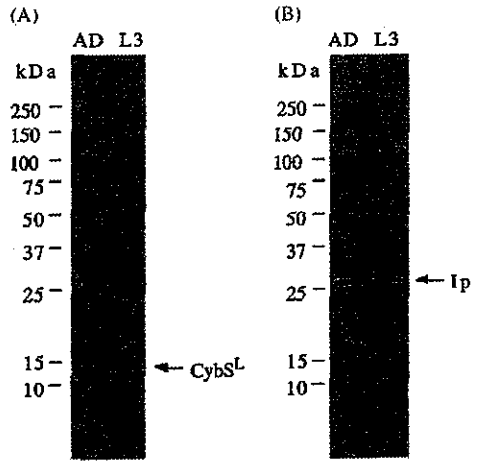

Fig. 6. Detection of the larva-specific CybS subunit using an anti-peptide antibody. Immunoblotting of mitochondria and complex IIs with a peptide antibody to (A) the larval CybS and (B) with a peptide antibody to the Ip. The larval complex II was purified from larval mitochondria as described in Section 2. AD, adult mitochondria (20 μg); L3, third stage larval mitochondria (20 μg).

II can function as a RQFR if electrons are transferred from rhodoquinol.

4. Discussion

The present study demonstrates that the larval form of CybS in the cytochrome *b* anchor subunits of complex II is distinct from CybS of the adult complex II. Northern analysis and immunoblotting showed specific expression of $CybS^L$ in the L3 stage and of $CybS^A$ in the adult stage. In contrast, the CybL subunit appears to be shared by these stage-specific isoforms of *A. suum* complex II. Thus, the both the Fp and CybS subunits are different in the larval and adult complex IIs, while the Ip and CybL subunits are shared by the two forms of complex II. Interestingly, our studies of purified enzymes showed that the both the adult and larval complex IIs catalyze RQFR activity, although subunit composition of larval complex II is different from that of adult enzyme. This is very different than the situation in bacteria wherein all of the subunits of the SQR and QFR complexes are unique.

While the primary structures of the soluble catalytic subunits, Fp and Ip, are highly conserved across species, the

sequence and the cofactor composition of the membrane anchor subunits vary. Based on their *b*-heme composition, membrane anchor domains have been grouped into three classes [41]. Type A SQR/QFR's contain two *b* hemes ligated to four conserved histidine residues and include QFR from *Wolinella succinogenes*. Type B complex II contains one *b* heme, and this includes most of the SQR's found in aerobic bacteria and mitochondria. Type C complex II, such as those of *Escherichia coli* QFR, contains no heme. Bacterial QFR's are either Type A or C, while their mitochondrial counterparts, such as the larval and adult complex IIs of *A. suum*, are Type B [41].

We found that the K_m values for rhodoquinol in the QFR and for ubiquinone in the SQR were similar for *A. suum* and for bovine complex IIs. However, the bovine enzyme had a lower QFR activity than the *A. suum* enzymes. This suggests that the quinone-binding pockets in complex IIs from the various organisms are similar. Recently, a sequence motif, aliphatic -$(x)_3$-H-$(x)_{2/3}$-(L/T/S) (where x represents any amino acid), was proposed by Fisher and Rich [42] for the prediction of quinone binding sites. A sequence fitting this motif, VSGLHRVT (residues 71–78 in D78157), immediately precedes transmembrane helix 1 in *A. suum* CybL. This region corresponds to residues 26–33 of SdhC in *E. coli* SQR, which is implicated in quinone binding [8,43], and to residues of *E. coli* FrdC that interact with menaquinone and inhibitors [44,45]. Furthermore, bovine CybL (QPs1) contains the sequence MSICHRGT (residues 67–74), which also fits the quinone binding motif, although this motif is absent in an isolated azido quinone-linked peptide (residues 142–169) that is located in the matrix side loop between transmembrane helices 2 and 3 [46]. Interestingly, the *C. elegans mev-1* mutant, whose phenotype is hypersensitivity to oxygen and a short life-span, harbors a substitution of glycine to glutamic acid in the correspond region, LSGFHRIS (residues 69–76) in CybL [47]. In this mutant, the SQR activity of complex II is much lower than in the wild-type strain, while SDH activity is comparable. Thus, it appears that transmembrane helix 1 of the CybL in complex II participates in quinone binding.

Such a quinone-binding motif cannot be readily recognized in the two *A. suum* CybS subunits [42]. Identification of the azido-quinone linked peptide and site-directed mutagenesis show that Ser-88 and Tyr-92 of bovine QPs3 (CybS), located at the end of transmembrane helix 1 toward the inner membrane space, are involved in quinone-binding [38,40]. As shown in Fig. 3, Ser-88 and Tyr-92 are not conserved in the two *A. suum* CybS proteins. Instead, hydrophilic amino acids would be located at the region that form hydrogen bonds to the carbonyl group of the benzoquinone ring in ubiquinone. Carboxin, which shows structural similarity to ubiquinone and is predicted to bind to the quinone-binding site, is a specific inhibitor of SQR from several different organisms. Resistance to carboxin is conferred by mutation of aspartic acid 89 to glycine in the SdhD of *Paracoccus denitrificans* complex II, a residue located in a predicted cytoplasmic loop connecting transmembrane helices 2 and 3 and close to the [3Fe–4S] cluster of Ip [48]. The adult and larval CybS of *A. suum* also have a conserved aspartic acid (Asp-91) in the predicted second loop (Figs. 3 and 7), although carboxin cause little inhibition of the SDH or SQR activities [1]. Since there is little information on cytochrome *b* from the Type B complex II, further biochemical and crystallographic studies are essential to understand the molecular mechanism of substrate binding and electron transfer by *A. suum* complex II. We recently isolated crystals of adult complex II and crystallographic studies are in progress (Osanai et al., unpublished observation).

Close relationship between the *A. suum* L3 and the *C. elegans* CybS genes was detected in the NJ tree with 80% bootstrap support (Fig. 4), while no significant support was obtained for the relationship in the ML analysis with a more realistic evolutionary model than that assumed for the estimation of the distance matrix used in the NJ analysis. If the tree shown in Fig. 4 were correct, then a gene duplication event should be assumed on the line leading to a common ancestor of nematodes. A loss of one gene might have occurred on the line leading to *C. elegans*. On the contrary, if the two *A. suum* genes were closely related with each other, a gene duplication event might have occurred on the line leading to *A. suum*, and one of the genes had adapted to an anaerobic condition and had used for an adult stage. Since no enough evolutionary information is resided in the CybS sequences, we cannot clearly settle this issue only by a present phylogenetic analysis.

Based on the FRD activities using methylviologen as an artificial electron donor, we show that the larval complex II catalyzes SQR in the aerobic respiration and that the adult complex II catalyzes RQFR in the anaerobic NADH-fumarate reductase system. Use of a synthetic rhodoquinone with short side-chain permitted a detailed kinetic analysis of the RQFR activity of the enzymes and revealed that both the larval and adult complex II have a higher RQFR and affinity for fumarate than the bovine complex II (Table 2). Similar results were observed using larval and adult mitochondria. Specifically, larval mitochondria had not only SQR activity but also high RQFR activity (80 nmol min^{-1} mg^{-1}). This RQFR activity is almost same as found in isolated adult mitochondria (Shinjyo et al., unpublished observation). This result, together with the low RQFR activity found in mitochondria from the free-living nematode *C. elegans* (6.5 nmol min^{-1} mg^{-1}), suggests that high RQFR activity is important for *A. suum* survival as a parasitic nematode. Such a high RQFR activity in L3 would favor parasite survival in the host small intestine where oxygen tension is very limited.

Why *A. suum* possesses two stage-specific complex IIs, even though both enzymes show high RQFR as well as SQR activity is uncertain. In addition, the differences between larval $Fp^L/CybS^L$ and adult $Fp^A/CybS^A$ are not obvious. One possible reason that we did not observe major differences between the larval and adult forms may be that we used a

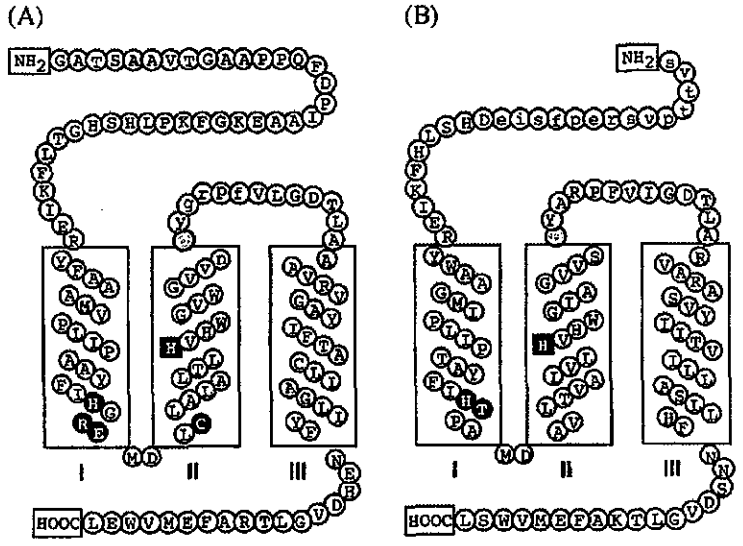

Fig. 7. Proposed topological model of the stage-specific CybS subunits in *A. suum* complex II (A) adult and (B) larval peptides. The closed circles indicate the hydrophilic amino acids located at the end of transmembrane helix 1 toward the inner membrane space, which might form hydrogen bonds with the carbonyl group of the benzoquinone ring of ubiquinone. The closed squares indicate a putative binding site for the heme *b* molecule. The gray circles indicate a conserved aspartic acid (D81 in the adult and D67 in the larval peptide) in a predicted cytoplasmic loop connecting transmembrane helices 2 and 3 close to the [3Fe–4S] cluster in the Ip. This corresponds to D89 in the SdhD of *P. denitrificans* which confers resistance to carboxin [48], and whose missense mutations cause paraganglioma (PGL) [50]. The amino acids shown in lower case indicate antibody epitopes, including vndygrpf (amino acids 79–86 in the adult peptide) as the epitope of a monoclonal antibody to the adult CybS (Fig. 1C), and svttpvsrepfsie (amino acids 1–14 in the larval peptide) used for preparation of a peptide-based antibody to the larval CybS (Fig. 6).

short-chain RQ with 2 isoprene units (RQ-2) for analyses of RQFR activity. Because RQ in *A. suum* mitochondria is RQ-9, it is possible that the RQFR activity of adult complex II is higher than larval enzyme under physiological conditions. Another possible reason is that the unique function of adult complex II is elevated FRD activity rather than a difference in RQFR activity. There is a high reducing equivalent in adult mitochondria due to the anaerobic conditions [6,15]. The FRD activity of adult complex II could help maintain the red-ox balance under these conditions by accepting electrons directly from soluble electron donors and transferring them to fumarate.

Dynamic rearrangement of the respiratory chain during life cycle of *A. suum* is one of the key elements of their adaptation. However, the regulatory mechanism responsible for the stage-specific expression of the genes in parasites is not well understood. Our present study clearly showed control of CybL and CybS expression at the level of transcription. Current research using the free-living nematode *C. elegans* has revealed that oxygen concentration, oxygen availability and oxidative stress can induce a variety of interesting phenotypes, including different life spans, and that the respiratory chain participates in the mechanism. A point mutation in CybL at residue 71 results in hypersensitivity to oxidative stress in the *C. elegans mev-1* strain [47]. On the other hand, we found that ubiquinone biosynthesis is dramatically altered in the long-lived mutant *clk-1* because the mitochondria contain the ubiquinone biosynthesis intermediate demethoxy ubiquinone (DMQ) instead of ubiquinone-9 [49]. These findings indicate that the respiratory chain helps respond to changes in the amount of oxygen in the environment (oxygen homeostasis). Interestingly, recent reports indicate that cytochrome *b* in complex II functions as an oxygen sensor [50]. Since *A. suum* shows dramatic changes in energy metabolism during its life cycle, it may be a good model system for investigating molecular mechanisms of biological adaptation to changing oxygen availability.

Acknowledgements

We would like to acknowledge Dr. T. Hashimoto (Institute of Statistical Mathematics) for the helpful advice in the phylogenetic analysis. We acknowledge Dr. Y. Watanabe, for useful discussions and critical reading of the manuscript. This work was supported by a Grant-in-Aid for Scientific Research on Priority Areas from the Ministry of Education, Science, Culture and Sport, Japan (13226015 and 13854011 to K.K., 13770123 to H.A.), Research on Emerging and Re-emerging Infectious Diseases from the Ministry of Health and Welfare (to K.K.). This study was also supported by "Pilot Applied Research Project for the Industrial Use of Space" of the National Space Development Agency of Japan (NASDA) and Japan Space Utilization Promotion Center (JSUP).

References

[1] Takamiya S, Kita K, Wang H, Weinstein PP, Hiraishi A, Oya H, et al. Developmental changes in the respiratory chain of *Ascaris* mitochondria. Biochim Biophys Acta 1993;1141:65–74.

[2] Kita K, Takamiya S. Electron-transfer complexes in *Ascaris* mitochondria. Adv Parasitol 2002;51:95–131.

[3] Kita K. Electron-transfer complexes of mitochondria in *Ascaris suum*. Parasitol Today 1992;8:155–9.

[4] Komuniecki R, Komuniecki PR. Aerobic–anaerobic transitions in energy metabolism during the development of the parasitic nematode *Ascaris suum*. In: Boothroyd JC, Komuniecki R, editors. Molecular approaches to parasitology. New York: Wiley-Liss, Inc.; 1995. p. 109–21.

[5] Kita K, Hirawake H, Takamiya S. Cytochromes in the respiratory chain of helminth mitochondria. Int J Parasitol 1997;27:617–30.

[6] Tielens AGM, Van Hellemond JJ. The electron transport chain in anaerobically functioning eukaryotes. Biochim Biophys Acta 1998;1365:71–8.

[7] Tielens AGM, Rotte C, van Hellemond JJ, Martin W. Mitochondria as we don't know them. Trends Biochem Sci 2002;27:564–72.

[8] Hägerhäll C. Succinate:quinone oxidoreductases. Variations on a conserved theme. Biochim Biophys Acta 1997;1320:107–41.

[9] Geenen PL, Bresciani J, Boes J, Pedersen A, Eriksen L, Fagerholm HP, et al. The morphogenesis of *Ascaris suum* to the infective third-stage larvae within egg. J Parasitol 1999;85:616–22.

[10] Takamiya S, Furushima R, Oya H. Electron transfer complexes of *Ascaris suum* muscle mitochondria. II. Succinate-coenzyme Q reductase (complex II) associated with substrate-reducible cytochrome b_{558}. Biochim Biophys Acta 1986;848:99–107.

[11] Kita K, Takamiya S, Furushima R, Ma YC, Oya H. Complex II is a major component of the respiratory chain in the muscle mitochondria of *Ascaris suum* with high fumarate reductase activity. Comp Biochem Physiol 1988;89B:31–4.

[12] Kita K, Takamiya S, Furushima R, Ma YC, Suzuki H, Ozawa T, et al. Electron-transfer complexes of *Ascaris suum* muscle mitochondria. III. Composition and fumarate reductase activity of complex II. Biochim Biophys Acta 1988;935:130–40.

[13] Saruta F, Kuramochi T, Nakamura K, Takamiya S, Yu Y, Aoki T, et al. Stage-specific isoforms of complex II (succinate-ubiquinone oxidoreductase) in mitochondria from the parasitic nematode, *Ascaris suum*. J Biol Chem 1995;270:928–32.

[14] Kuramochi T, Hirawake H, Kojima S, Takamiya S, Furushima R, Aoki T, et al. Sequence comparison between the flavoprotein subunit of the fumarate reductase (complex II) of the anaerobic parasitic nematode, *Ascaris suum* and the succinate dehydrogenase of the aerobic, free-living nematode, *Caenorhabditis elegans*. Mol Biochem Parasitol 1994;68:177–87.

[15] Kita K, Hirawake H, Miyadera H, Amino H, Takeo S. Role of complex II in anaerobic respiration of the parasite mitochondria from *Ascaris suum* and *Plasmodium falciparum*. Biochim Biophys Acta 2002;1553:123–39.

[16] Amino H, Wang H, Hirawake H, Saruta F, Mizuchi D, Mineki R, et al. Stage-specific isoforms of *Ascaris suum* complex II: the fumarate reductase of the parasitic adult and the succinate dehydrogenase of free-living larvae share a common iron–sulfur subunit. Mol Biochem Parasitol 2000;106:63–76.

[17] Takamiya S, Kita K, Matsuura K, Furushima R, Oya H. Oxidation–reduction potentials of cytochromes in *Ascaris* muscle mitochondria: high-redox potential cytochrome b_{558} in complex II. Biochem Int 1990;21:1073–80.

[18] Yu L, Xu J, Haley PE, Yu C. Properties of bovine heart mitochondrial cytochrome b_{560}. J Biol Chem 1987;262:1137–43.

[19] Kita K, Mizuchi D, Wang H, Takamiya S, Aoki T, Kojima S. cDNA sequence of three cysteine-rich clusters in the iron–sulfur subunit of complex II (succinate-ubiquinone oxidoreductase) from *Caenorhabditis elegans* determined by automated DNA sequencer. Electrophoresis 1992;13:506–11.

[20] Saruta F, Hirawake H, Takamiya S, Ma Y-C, Aoki T, Sekimizu K, et al. Cloning of a cDNA encoding the small subunit of cytochrome b_{558} (CybS) of mitochondrial fumarate reductase (complex II) from adult *Ascaris suum*. Biochim Biophys Acta 1996;1276:1–5.

[21] Matsudaira P. Sequence from picomole quantities of proteins electroblotted onto polyvinylidene difluoride membranes. J Biol Chem 1987;262:10035–8.

[22] Rosenfeld J, Capdevielle J, Guillemot JC, Ferrara P. In-gel digestion of proteins for internal sequence analysis after one- or two-dimensional gel electrophoresis. Anal Biochem 1992;203:173–9.

[23] Shevchenko A, Wilm M, Vorm O, Matthias M. Mass spectrometric sequencing of proteins from silver-stained polyacrylamide gel. Anal Chem 1996;68:850–8.

[24] Chomczynski P, Sacchi N. Single-step method of RNA isolation by acid guanidinium thiocynate–phenol–chloroform extraction. Anal Biochem 1987;162:156–9.

[25] Nilsen T, Shambaugh J, Denker J, Chubb G, Faser C, Putnam L, et al. Characterization and expression of a spliced leader RNA in the parasitic nematode *Ascaris lumbricoides* var. *suum*. Mol Cell Biol 1989;9:3543–7.

[26] Thompson JD, Gibson TJ, Plewniak F, Jeanmougin F, Higgins DG. The CLUSTAL_X windows interface: flexible strategies for multiple sequence alignment aided by quality analysis tools. Nucl Acids Res 1997;25:4876–82.

[27] Yang Z. PAML: a program package for phylogenetic analysis by maximum likelihood. Comput Appl Biosci 1997;13:555–6.

[28] Shimodaira H, Hasegawa M. CONSEL: for assessing the confidence of phylogenetic tree selection. Bioinformatics 2001;17:1246–7.

[29] Ausubel FM, Brent R, Kingston RE, Moore DD, Seidman JG, Smith JA, et al. Current protocols in molecular biology. New York: Greene Publishing Associates and Wiley-Interscience; 1987.

[30] Kita K, Vibat CR, Meinhardt S, Guest JR, Gennis RB. One-step purification from *Escherichia coli* of complex II (succinate: ubiquinone oxidoreductase) associated with succinate-reducible cytochrome b_{556}. J Biol Chem 1989;264:2672–7.

[31] Omura S, Miyadera H, Ui H, Shiomi K, Yamaguchi Y, Masuma R, et al. An antihelmintic compound, nafuredin, shows selective inhibition of complex I in helminth mitochondria. Proc Natl Acad Sci USA 2001;98:60–2.

[32] Lowry OH, Rosebrough NJ, Farr AL, Randall RJ. Protein measurement with the folin phenol reagent. J Biol Chem 1951;193:265–75.

[33] Towbin H, Staehelin T, Gordon J. Electrophoretic transfer of proteins from polyacrylamide gels to nitrocellulose sheets: procedure and some applications. Proc Natl Acad Sci USA 1979;76:4350–4.

[34] The *C. elegans* Sequencing Consortium. Genome sequence of the nematode *C. elegans*: a platform for investigating biology. Science 1998;282:2012–8.

[35] Hurt EC, Van Loon AP. How proteins find mitochondria and intramitochondrial compartments. Trends Biochem Sci 1986;11:204–7.

[36] Gennis RB. Biomembranes: molecular structure and function. New York: Springer-Verlag; 1989.

[37] Hirawake H, Taniwaki M, Tamura A, Kojima S, Kita K. Cytochrome *b* in human complex II (succinate-ubiquinone oxidoreductase): cDNA cloning of the components in liver mitochondria and chromosome assignment of the genes for the large (SDHC) and small (SDHD) subunits to 1q21 and 11q23. Cytogenet Cell Genet 1997;79:132–8.

[38] Shenoy SK, Yu L, Yu CA. The smallest membrane anchoring subunit (QPs3) of bovine heart mitochondrial succinate-ubiquinone reductase. J Biol Chem 1997;272:17867–72.

[39] Bullis BL, Lemire BD. Isolation and characterization of the *Saccharomyces cerevisiae* SDH4 gene encoding a membrane anchor subunit of succinate dehydrogenase. J Biol Chem 1994;269:6543–9.

[40] Shenoy SK, Yu L, Yu CA. Identification of quinone-binding and heme-ligating residues of the smallest membrane anchoring subunit

(QPs3) of bovine heart mitochondrial succinate:ubiquinone reductase. J Biol Chem 1999;274:8717–22.
[41] Hägerhäll C, Hederstedt L. A structural model for the membrane-integral domain of succinate:quinone oxidoreductases. FEBS Lett 1996;389:25–31.
[42] Fisher N, Rich PR. A motif for quinone binding sites in respiratory and photosynthetic systems. J Mol Biol 2000;296:1153–62.
[43] Yang X, Yu L, He D, Yu CA. The quinone-binding site in succinate-ubiquinone reductase from *Escherichia coli*. J Biol Chem 1998;273:31916–23.
[44] Iverson TM, Luna-Chavez C, Cecchini G, Rees DC. Structure of *Escherichia coli* fumarate reductase respiratory complex. Science 1999;284:1961–6.
[45] Iverson TM, Luna-Chavez C, Croal LR, Cecchini G, Rees DC. Crystallographic studies of the *Escherichia coli* quinol-fumarate reductase with inhibitors bound to the quinol-binding site. J Biol Chem 2002;277:16124–30.
[46] Lee GY, He DY, Yu L, Yu CA. Identification of the ubiquinone-binding domain of QPs1 of succinate-ubiquinone reductase. J Biol Chem 1995;270:6193–8.
[47] Ishii N, Fujii M, Hartman PS, Tsuda M, Yasuda K, Senoo-Matsuda N, et al. A mutation in succinate dehydrogenase cytochrome *b* causes oxidative stress and ageing in nematodes. Nature 1998;394:694–7.
[48] Matsson M, Ackrell BAC, Cochran B, Hederstedt L. Carboxin resistance in *Paracoccus denitrificans* conferred by a mutation in the membrane-anchor domain of succinate:quinone reductase (complex II). Arch Microbiol 1998;170:27–37.
[49] Miyadera H, Amino H, Hiraishi A, Taka H, Murayama K, Miyoshi H, et al. Altered quinone biosynthesis in the long-lived clk-1 mutants of *Caenorhabditis elegans*. J Biol Chem 2001;276:7713–6.
[50] Baysal BE, Ferrell RE, Willett-Brozick JE, Lawrence EC, Myssiorek D, Bosch A, et al. Mutations in SDHD, a mitochondrial complex II gene, in hereditary paraganglioma. Science 2000;287:848–51.
[51] Wood D, Darlison MG, Wilde RJ, Guest JR. Nucleotide sequence encoding the flavoprotein and hydrophobic subunits of the succinate dehydrogenase of *Escherichia coli*. Biochem J 1984;222:519–34.
[52] Cole ST. Nucleotide sequence coding for the flavoprotein subunit of the fumarate reductase of *Escherichia coli*. Eur J Biochem 1982;122:479–84.

ACADEMIC PRESS

Available online at www.sciencedirect.com

SCIENCE DIRECT®

Archives of Biochemistry and Biophysics 413 (2003) 253–261

ABB

www.elsevier.com/locate/yabbi

Heterologous expression of *Ascaris suum* cytochrome b_5 precursor protein: a histidine-tagged full-length presequence is correctly processed to transport the mature protein to the periplasm of *Escherichia coli*

Shinzaburo Takamiya,[a,*] Hiroshi Yamasaki,[a,1] Muneaki Hashimoto,[b] Hikari Taka,[c] Kimie Murayama,[c] Mitsuo Tagaya,[b] and Takashi Aoki[a]

[a] *Department of Molecular and Cellular Parasitology, Juntendo University School of Medicine, Hongo 2-1-1, Bunkyo-ku, Tokyo 113-8421, Japan*
[b] *Laboratory of Molecular Cell Biology, School of Life Science, Tokyo University of Pharmacy and Life Science, 1432-1 Horinouchi, Hachioji, Tokyo 192-0392, Japan*
[c] *Central Laboratory of Medical Sciences, Juntendo University School of Medicine, Hongo 2-1-1, Bunkyo-ku, Tokyo 113-8421, Japan*

Received 8 January 2003, and in revised form 26 February 2003

Abstract

The cytochrome b_5 of the body wall of adult *Ascaris suum*, a porcine parasitic nematode, is a novel type of cytochrome b_5. It is a soluble protein that lacks the COOH-terminal membrane-anchoring domain found in erythrocyte cytochrome b_5, but possesses an NH_2-terminal extension (presequence) of 30 amino acids that are missing from the 82-residue protein purified from the nematode tissues [Yu, Y., Yamasaki, H., Kita, K., and Takamiya, S., 1996, Arch. Biochem. Biophys. 328, 165–172]. The nematode cytochrome b_5 is, therefore, probably synthesized as a precursor protein whose presequence is cleaved to form a mature protein, but the localization of the mature protein is still unknown. To investigate the processing of the putative precursor protein, the wild-type precursor of nematode cytochrome b_5 with a complete presequence (b5wt) and its NH_2 terminus-truncated derivatives, b5Δ18 and b5Δ28, with 18 and 28 residues deleted, respectively, were expressed using pET-28a(+) vector in *Escherichia coli*. As expected, all transformants, tb5wt, tb5Δ18, and tb5Δ28, produced recombinant proteins with a histidine-tagged NH_2-terminal extension. However, only the recombinant protein with the full-length presequence, produced in tb5wt, was correctly processed and transported to the periplasm, from which the majority of the induced product was purified as a mature protein chemically and functionally identical to the native protein purified from the nematode body wall. These results clearly show that the nematode histidine-tagged presequence functions as a signal peptide in *E. coli*.

Keywords: Cytochrome b_5 precursor; Signal peptide; *Ascaris suum*

Cytochrome b_5, a hemoprotein electron carrier, is ubiquitously distributed in bacteria [1], yeast [2], fungi [3], plants [4,5], invertebrates [6–12], and vertebrates [13–16] and is involved in a variety of biological redox reactions [17–19]. There are two forms of cytochrome b_5, isolated membrane-bound forms and soluble forms, which are localized in microsomes and erythrocytes, respectively. The microsomal cytochrome b_5 is composed of two distinct domains, a hydrophilic NH_2-terminal domain of about 100 amino acids and a hydrophobic COOH-terminal domain of about 30 amino acids. The NH_2-terminal domain contains a protoheme and participates in the electron transfer function, whereas the COOH-terminal domain has two portions, a hydrophobic membrane-anchoring portion (about 20 residues) and a terminal hydrophilic portion (about 10 residues) containing sufficient information for targeting the cytochrome to the endoplasmic reticulum

* Corresponding author. Fax: +81-3-5800-0476.
E-mail address: stakamiy@med.juntendo.ac.jp (S. Takamiya).
[1] Present address: Department of Parasitology, Asahikawa Medical College, Midorigaoka Higashi 2-1-1-1, Asahikawa 078-8510, Japan.

0003-9861/03/$ - see front matter © 2003 Elsevier Science (USA). All rights reserved.
doi:10.1016/S0003-9861(03)00124-3

membrane [20]. Cytochrome b_5 serves as an electron carrier between microsomal NAD(P)H cytochrome b_5 reductase and various microsomal enzymes including stearyl CoA desaturase [21] and P-450s [19].

The erythrocyte cytochrome b_5 is a hydrophilic hemoprotein composed of 97 amino acids, whose primary structure is identical to that of the catalytic domain of the microsomal form except that the COOH terminus (residue 97) is replaced by a different amino acid residue in porcine, rabbit, and human proteins [22,23]. In any case, the erythrocyte cytochrome b_5 contains the common catalytic domain structure and lacks the COOH-terminal membrane-anchoring domain to allow the protein to be soluble in red cells. The erythrocyte cytochrome b_5 is involved in the NADH-dependent reduction of methemoglobin to hemoglobin [24].

We previously isolated a novel type of cytochrome b_5 from the body wall of adult *Ascaris suum*, a porcine parasitic nematode [25]. This cytochrome b_5 was coextracted with mitochondrial cytochrome *c* and demonstrated to be a soluble protein of 82 amino acids; no equivalent of the COOH-terminal hydrophobic domain of the microsomal form was found. Surprisingly, cloning the cDNA encoding *A. suum* cytochrome b_5 revealed an NH_2-terminal extension (presequence) of 30 amino acids, which was not found in the protein purified from the nematode body wall. The cytochrome b_5 is probably synthesized as a precursor protein of 112 amino acids, and the presequence is cleaved later to form a mature cytochrome b_5 of 82 amino acids. However, the putative precursor protein could not be detected by immunoblotting using anti-*A. suum* cytochrome b_5 antibody [25]. Furthermore, the localization of the mature cytochrome b_5 in the *A. suum* body wall remains unclear; immunoblotting analyses of subcellular fractions did not show its presence in any subcellular organelle, including the nucleus, mitochondria, and microsome fractions, but it was found in the cytoplasmic fraction (data not shown). Thus, the site where the presequence is cleaved and the organelle to which the mature protein is targeted are not yet known.

In this study, the putative precursor protein of nematode cytochrome b_5 and its NH_2 terminus-truncated derivatives were expressed in *Escherichia coli* with the intent of preparing possible substrates for studying processing proteases in *A. suum*. Surprisingly, the recombinant full-length precursor protein, but not its truncated derivatives, was processed correctly in the bacteria and transported to the periplasm to form a mature cytochrome b_5 identical to the protein purified from the *A. suum* body wall. In this communication, we describe the properties of the processed cytochrome b_5 and discuss the probable function of the presequence based on the behavior of putative precursor proteins in *E.coli*.

Materials and methods

Construction of expression plasmids and transformants

A 563-bp cDNA clone of *A. suum* cytochrome b_5, previously isolated, consists of an open reading frame containing three putative initiator codons (in-phase ATG codons for methionine) [25]. These correspond to the 1st, 19th, and 29th methionines in the presequence (Fig. 1A). Although the scanning model postulated by Kozak [26] predicts that the first ATG codon in a favorable context is the initiator codon, we considered the possibility that the second or third ATG codon functions as the initiator codon; there are some exceptions depending on the downstream secondary structure. Thus, three cDNAs encoding *A. suum* cytochromes b_5, one possessing the full-length presequence starting from

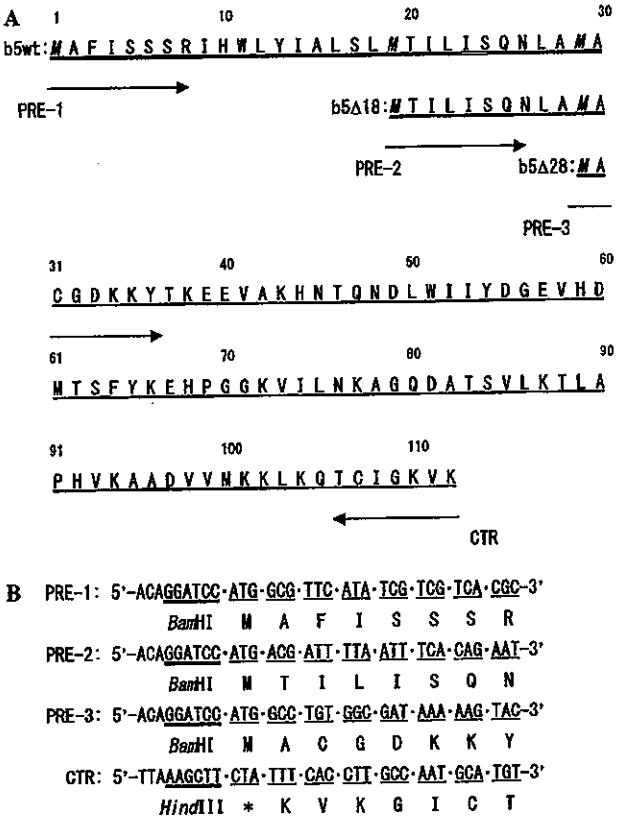

Fig. 1. Amino acid sequences of the wild-type precursor of *A. suum* cytochrome b_5 (b5wt) and its NH_2 terminus-truncated derivatives (b5Δ18 and b5Δ28) (A) and nucleotide sequences of primers to synthesize cDNAs encoding b5wt, b5Δ18, and b5Δ28 (B). (A) The portions of putative presequences and the mature protein (common) are double-underlined and thickly underlined, respectively. Three methionines in the presequence are shown by italic letters. The amino acid sequences of the designed primers, PRE-1, -2, -3, and CTR, and their orientations are shown by underlining with arrows. (B) Recognition sites for restriction enzymes are double-underlined. Sense and antisense codons are underlined with corresponding amino acids and stop signal (*) shown below.

the first methionine and the other two possessing truncated presequences starting from the second and the third methionines, which are the 19th and 29th residues from the NH_2 terminus of the presequence, respectively, were amplified by PCR[2] using the cDNA encoding the nematode cytochrome b_5 as a template. To produce these cDNAs and introduce them into vectors, three forward oligonucleotide primers appended with a *Bam*HI recognition site, PRE-1, -2, and -3, and a reverse primer appended with a *Hin*dIII site, CTR, were synthesized (Fig. 1B). PCR was performed using Ampli*Taq* DNA polymerase (Perkin–Elmer) for 35 cycles of 1 min at 95 °C, 1 min at 55 °C, and 2 min at 72 °C. These PCR products were subcloned into pT7Blue T-vector (Novagen, USA) and sequenced to confirm the three cDNAs, one encoding the wild-type cytochrome b_5 with a full-length presequence consisting of 30 amino acid residues and a mature region consisting of 82 residues (b5wt; Fig. 1A) and two encoding cytochromes b_5 with truncated presequences lacking the NH_2-terminal 18 and 28 amino acid residues (b5Δ18 and b5Δ28; Fig. 1A). These cDNAs were inserted into pET-28a(+) expression vector (Novagen) and designated pb5wt, pb5Δ18, and pb5Δ28. Each construct was then introduced into BL21(DE3) *E. coli* strain (Novagen), producing three transformants designated tb5wt, tb5Δ18, and tb5Δ28.

Growth of transformants

Transformed cells were precultured overnight at 37 °C in 2 ml of Luria–Bertani medium containing 30 μg/ml kanamycin. The culture was then inoculated into 120–250 ml of medium supplemented with 30 μg/ml of kanamycin and the medium was shaken aerobically at 37 °C. When the cell density reached to 0.6–0.8 O.D. at 600 nm, IPTG (1 mM in final conc.) was added to the culture to induce expression of proteins. The culture was shaken overnight at 25 °C and centrifuged at 5000*g* for 10 min to harvest the cells.

Subcellular fractionation of bacteria

The bacteria harvested from 120 ml of culture were resuspended in 20 ml of medium containing 30 mM Tris–HCl, pH 8.0, 0.61 M sucrose, 0.5 mM Na_2EDTA, and 0.25 mg/ml of lysozyme. The suspension was left at 20 °C for 20 min and centrifuged at 15,000*g* for 20 min to give the periplasmic fraction in the supernatant and a pellet of spheroplasts. To release cytoplasmic proteins, the spheroplasts were resuspended in 7 ml of 10 mM Tris–HCl, pH 8.0, containing 2 mM Na_2EDTA and left to stand at 20 °C for 30 min. Since the release of DNA disturbs fractionation, $MgCl_2$ (4 mM final conc.) and DNase I (200 μg/ml) were added to the suspension. The mixture was left at 4 °C for 30 min and centrifuged at 424,000*g* for 30 min (Beckman Optima Ultracentrifuge) to yield the cytoplasmic fraction in the supernatant and the membrane fraction in the pellet. The pellet was suspended in 9 ml of 10 mM Tris–HCl, pH 8.0.

Preparation of the microsomal fraction of A. suum

All operations were carried out at 4 °C. Fresh body wall (26–37 g) was cut into small pieces with scissors and homogenized with a Physcotron (NITI-ON Co.) at maximum output for 1 min following the addition of 10 volumes of 0.25 M sucrose containing 3 mM $MgCl_2$. The homogenate was filtered through a layer of nylon cloth (100 mesh) and centrifuged at 900*g* for 5 min. The pellet was discarded. The supernatant was then centrifuged at 9100*g* for 7 min. The precipitate was put aside for the preparation of mitochondria. The resultant supernatant was centrifuged at 106,000*g* for 1.5 h to yield the microsomal fraction as a loosely packed pellet. The pellet was suspended in 40 ml of 1.15% KCl solution and centrifuged at 106,000*g* for 1 h. The final pellet was dispersed in a small volume of KCl solution using a Potter–Elvehjem-type homogenizer.

Purification of processed cytochrome b_5 from cells transformed with pb5wt

Cells harvested from 250 ml of culture were suspended in 2 ml of 20 mM sodium phosphate buffer, pH 7.6, containing 1 mM PMSF. The suspension was frozen at −20 °C for 1 h and thawed at room temperature. After stirring the suspension with a glass rod, the suspension was again frozen at −20 °C. This freeze–thaw cycle was carried out three times in total. To the final thawed suspension was added 1 ml of the same buffer, and the mixture was centrifuged at 424,000*g* for 30 min. The resulting red-colored supernatant, following the addition of a few grains of crystal potassium ferricyanide to oxidize cytochrome b_5, was dialyzed in a cold room against 300 ml of 20 mM sodium phosphate buffer, pH 7.6, for 3 h and overnight after one change of buffer. The dialyzed sample was loaded onto a CM-500 cellulofine (Seikagaku Kogyo, Co.) columm (1 × 13 cm), previously equilibrated with the same buffer, and eluted with a linear gradient of NaCl (0–0.5 M) in a total volume of 100 ml. The fractions containing cytochrome b_5 were combined and concentrated through a YM-1 membrane (Amicon, Millipore Co.).

[2] *Abbreviations used:* PCR, polymerase chain reaction; IPTG, isopropyl-β-D-thiogalactopyranoside; PMSF, phenylmethlysulfonyl fluoride; ESI, electrospray ionization; SDS–PAGE, sodium dodecylsulfate polyacrylamide gel electrophoresis; DCIP, 2,6-dichlorophenolindophenol; UQ, ubiquinone.

Purification of cytochrome b_5 from the body wall of A. suum

Native cytochrome b_5 was purified from the body wall of adult *A. suum* as previously described [25].

Enzyme assays

Alkaline phosphatase activity was determined at 30 °C by monitoring the increase in the absorbance at 410 nm due to the accumulation of free *p*-nitrophenol cleaved by enzymatic hydrolysis from *p*-nitrophenol phosphate [27]. The reaction was initiated by the addition of the enzyme and the increase in absorbance at 410 nm was recorded against a reference cuvette lacking the substrate and enzyme. An extinction coefficient at 410 nm at pH 8.2 of $1.62 \times 10^{-4}\,M^{-1}\,cm^{-1}$ was used for calculation.

Isocitrate dehydrogenase was spectrophotometrically assayed at 25 °C by monitoring the rate of NADPH formation [28]. The medium contained the enzyme, 50 mM triethanolamine, pH 7.4, 4 mM $MnSO_4$, 0.33 mM $NADP^+$, and 6 mM sodium isocitrate in a total volume of 1 ml. The reaction was initiated by the addition of the enzyme.

Succinate–ubiquinone reductase activity was determined at 25 °C by monitoring the rate of ubiquinone-dependent DCIP (Sigma) reduction [29]. The reaction mixture contained enzyme samples, 0.1 M potassium phosphate, pH 7.4, 0.3 mM EDTA, 0.053 mM DCIP, 2 mM potassium succinate, and 25 μM ubiquinone-2 in 1 ml. The reaction was started by the addition of succinate and the decrease of absorbance at 600 nm was recorded. The rate of ubiquinone-dependent DCIP reduction was obtained by subtracting the rate in the absence of ubiquinone from that in the presence of the quinone. A molar extinction coefficient of $21\,mM^{-1}\,cm^{-1}$ at 600 nm for DCIP was used for calculation.

Spectrophotometry

All absorption spectra were recorded on a dual-wavelength spectrophotometer (Model 557; Hitachi, Ltd.). The amounts of cytochrome b_5 in the subcellular fractions of transformants were calculated from reduced-minus-oxidized difference spectra recorded at room temperature as previously reported [30]. The difference extinction coefficients ($\Delta\varepsilon$) at 424 and 559 nm used for calculation were 107.7 and $14.4\,mM^{-1}\,cm^{-1}$, respectively, both of which were determined in the present study. The contributions of endogenous cytochromes were calibrated using subcellular fractions of host *E. coli* BL2(DE3).

SDS–PAGE and immunoblotting

To separate cytochrome b_5 derivatives with slightly different molecular masses, a high-resolution gel electrophoresis was carried out except that 10-cm-long gels were used instead of 25-cm-long gels [31]. After electrophoresis, blotting was performed according to the method of Towbin et al. [32]. Antiserum against *A. suum* cytochrome b_5 [25] was further purified through Protein A Sepharose 4 Fast Flow (Pharmacia) according to the manufacture's protocol to yield an IgG fraction. A Western–light chemiluminescent detection system (Tropix) was used for detection.

Determination of molecular mass

The molecular mass of the processed cytochrome b_5 was determined by electrospray ionization (ESI) mass spectrometry using a Finnigan Mat SSQ-7000 mass spectrometer as previously described [25].

NH_2-terminal sequencing of proteins

Proteins were separated by SDS–PAGE and electroblotted to polyvinylidene difluoride (Immobilon-P^{SQ}; Millipore Co.) membranes in 10 mM 3-(cyclohexylamino)-1-propanesulfonic acid (Sigma), pH 11. Protein bands were visualized with Coomassie brilliant blue R-250 staining, air-dried, and cut out. Samples were then analyzed by sequencing on an Applied Biosystems 470A sequencer with an online 120A analyzer.

Other methods

Absorption coefficients and heme contents of native and processed cytochromes b_5 were determined as previously reported [33] using a value of $32.0\,mM^{-1}\,cm^{-1}$ for the molar coefficient of the α maximum at 557 nm of pyridin–hemochromogen. Protein was determined by the modification of the Lowry method described by Markwell et al. [34] with bovine serum albumin as the standard.

Results

Expression of putative precursor proteins

All constructed plasmids, pb5wt, pb5Δ18, and pb5Δ28, were shown visually to transform the host cells; upon IPTG induction, both the transformants tb5wt and tb5Δ28 appeared deep pink, whereas the transformant tb5Δ18 was less pink (data not shown). All transformants were expected to produce the recombinant proteins carrying an additional histidine tag at each NH_2 terminus. Temperature was noted to affect the growth of transformants. When IPTG induction was carried at 37 °C, as on preculture, the yield of cells was very poor. The reason for this is not clear, but the rapid accumulation of recombinant proteins may be toxic for

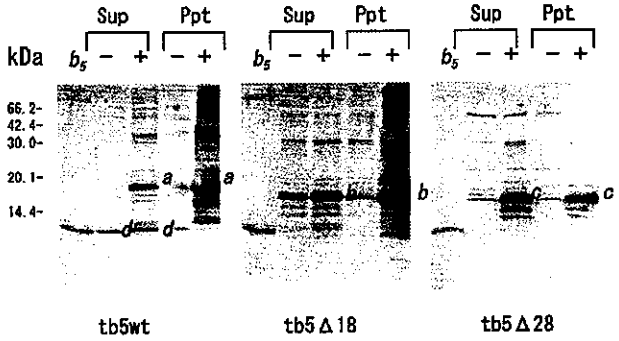

Fig. 2. Analysis of recombinant proteins by immunoblotting. Transformed cells, tb5wt, tb5Δ18, and tb5Δ28, were cultured at 37 °C, each in 5 ml of Luria–Bertani medium containing 30 μg/ml of kanamycin. When the cell density reached 0.6–0.8 O. D. at 600 nm, the culture was divided into two halves. IPTG (1 mM final conc.) was added to one of the halves (+) and the other received no addition (–). The two cultures were shaken at 25 °C for 2 h, after which 1.5 ml of the culture was centrifuged at 5000*g* for 10 min to harvest cells. The supernatants were discarded and the pellets were resuspended in 0.3 ml of ice-cold phosphate buffer (20 mM potassium phosphate, pH 7.4) in small glass vials. The suspended cells were lysed at 4 °C in a sonicater (bath type) until the turbidity was diminished. The lysate was centrifuged at 6000*g* for 10 min at 4 °C. The supernatant and pellet, resuspended in a small volume of a phosphate-buffered saline, were used as Sup and Ppt fractions for immunoblotting analysis as described under Materials and methods; b_5 indicates *A. suum* cytochrome b_5 (2 μg) purified from the nematode body wall. The protein contents loaded were as follows: tb5wt (Sup, 20.2 μg each; Ppt, 20.3 μg each) tb5Δ18 (Sup, 20.8 μg each; Ppt, 20.5 μg each), and tb5Δ28 (Sup, 29.0 μg each; Ppt, 28.3 μg each).

cell growth. Thus, a lower temperature, 25 °C, was employed for IPTG induction.

To analyze recombinant precursor proteins, lysates of three transformants, tb5wt, tb5Δ18, and tb5Δ28, cultured on a small scale in the presence (+) or absence (–) of IPTG, were probed with anti-*A. suum* cytochrome b_5 antibody (Fig. 2). In the presence of IPTG, the major stained bands, shown as bands *a* of tb5wt, *b* of tb5Δ18, and *c* of tb5Δ28 in both the Sup (+) and Ppt (+) lanes, were much more remarkable than those in the absence of IPTG. The molecular weights of these major bands are higher than that of native *A. suum* cytochrome b_5 in the order of tb5wt, tb5Δ18, and tb5Δ28 (more clearly seen in Fig. 3, bands *a*, *b*, and c). These results, as we expected, indicate that the recombinant proteins were well induced with IPTG. To our surprise, however, a clearly stained band with a molecular weight the same as that of native cytochrome b_5 was detected in the lysate of tb5wt (band *d* in Fig. 2), but not in the lysates of either tb5Δ18 or tb5Δ28. This suggests the possibility that the recombinant precursor protein produced in tb5wt was correctly processed in the host cells. If this is the case, some interesting questions arise. First, are the recombinant and processed proteins associated with protoheme or apoproteins? Second, where is the processed protein targeted in the host cells? Third, what is the role of the presequence in the targeting process?

Distribution of recombinant precursor proteins in the subcellular fractions of transformants tb5wt, tb5Δ18, and tb5Δ28

It is important to know the distribution of the recombinant and processed proteins in the host cells because their efficient purification greatly depends on where they are mainly localized and how they exist, i.e., in soluble or insoluble forms. Thus, transformants tb5wt, tb5Δ18, and tb5Δ28 were cultivated on a large scale (120 ml) in the presence of IPTG to prepare periplasmic, cytosolic, and membrane fractions. These fractions were analyzed in detail by SDS–PAGE (Fig. 3A) and immunoblotting using anti-*A. suum* cytochrome b_5 antibody (Fig. 3B). The recombinant full-length

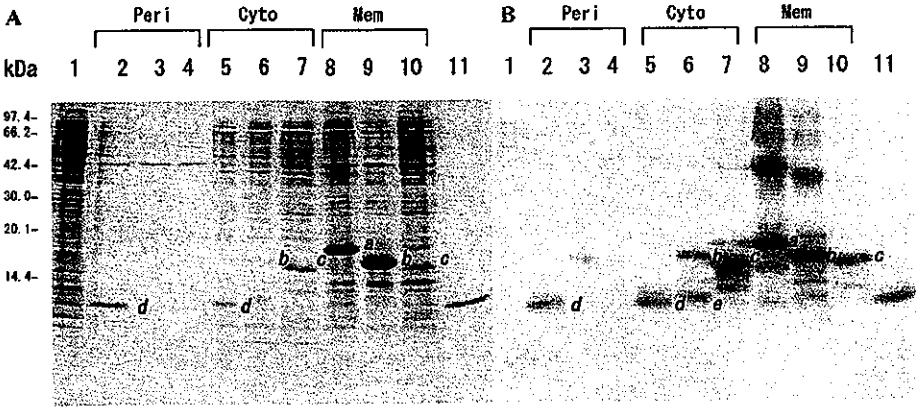

Fig. 3. SDS–PAGE analysis of subcellular fractions from transformants tb5wt, tb5Δ18, and tb5Δ28. (A) Coomassie brilliant blue-stained gel; (B) blotted sheet probed with anti-*A. suum* cytochrome b_5 antibody. Lane 1, *E. coli* BL21(DE3) homogenate, 50 μg; lanes 2–4, periplasmic fractions from tb5wt, tb5Δ18, and tb5Δ28, respectively (10 μg of protein was loaded); lanes 5–7, cytoplasmic fractions from tb5wt, tb5Δ18, and tb5Δ28, respectively (19.4 μg of protein was loaded); lanes 8–10 membrane fractions from transformants b5wt, b5Δ18, and b5Δ28, respectively (50 μg of protein was loaded); lane 11, cytochrome b_5 purified from *A. suum* body wall (1.6 μg).

precursor protein of tb5wt was shown to be exclusively localized in the membrane fraction (Figs. 3A and B, band *a* in lane 8); no corresponding band was detected in either the periplasmic or the the cytoplasmic fractions. However, the recombinant truncated-precursor protein of tb5Δ18 was shown to be mainly localized in the membrane fraction, but partly distributed in the cytoplasmic fraction (Figs. 3A and B, band *b* in lanes 6 and 9) also. The cytoplasmic distribution of the recombinant protein was more remarkable in the case of tb5Δ28; its amount was larger in the cytoplasmic fraction than in the membrane fraction (Figs. 3A and B, band *c* in lanes 7 and 10).

Most intriguingly, some processed products were detected in the periplasmic and cytoplasmic fractions of tb5wt and tb5Δ18 (Figs. 3A and B, band *d* in lanes 2 and 5; Fig. 3B, band *e* in lane 6). Only the recombinant full-length precursor protein was demonstrated to be processed and targeted to the periplasm (Figs. 3A and B, band *d* in lane 2). In fact, the NH_2-terminal sequence of the band *d* protein in lane 2 was shown to be CGDKKYTKEEVAKHNTQNDL-, identical to that of native *A. suum* cytochrome b_5 up to the 20th residue. The NH_2-terminal sequence of the band *a* protein was also determined to be GSSHHHHHHSSGLVPRGSH MASMTGGQQMGRGS*MAF*-, confirming that the recombinant protein indeed has its histidine-tagged extension, which includes a thrombin cleavage site (underlined), T 7 tag (double-underlined), and a full-length presequence starting from the first methionine (italic letters). To study the distribution of cytochrome b_5 in the subcellular fractions as the holoprotein, the cytochrome content was determined spectrophotometrically based on the specific absorption of cytochrome b_5 and the percentage total recovery of marker enzymes for the fractions, i.e., alkaline phosphatase, isocitrate dehydrogenase, and succinate UQ reductase for the periplasmic, cytoplasmic, and membrane fractions, respectively (Table 1). Although fractionation between the periplasm and the cytoplasm appeared to be incomplete, the distribution of cytochrome b_5 as a holoprotein was demonstrated, answering the first question above. The total yield of recombinant cytochrome b_5 is 1.5- and 1.8-fold higher in transformant tb5wt (166 nmol) than in tb5Δ28 (106 nmol) and tb5Δ18 (89 nmol), respectively. It should be stressed that the correctly processed protein with heme was recovered at about 70% in the periplasmic fraction of the tb5wt transformant.

Table 1
Distribution of cytochrome b_5 and marker enzymes in transformants tb5wt, tb5Δ18, and tb5Δ28[a]

Fraction	Alkaline phospatase			Isocitrate dehydrogenase (% of total revovery)			Succinate UQ reductase			Cytochrome b_5 (nmol)		
	tb5wt	tb5Δ18	tb5Δ28	tb5wt	tb5Δ18	tb5Δ28	tb5wt	tb5Δ18	tb5Δ28	tb5wt	tb5Δ18	tb5Δ28
Periplasm	74.0 ± 6.9	73.5 ± 2.5	61.5 ± 4.2	3.1 ± 5.4	0.0	0.0	0.0	0.0	0.0	125.4 ± 5.5	0.0	0.0
Cytoplasm	22.7 ± 1.7	26.5 ± 2.5	38.5 ± 4.5	96.9 ± 5.4	92.1 ± 15.8	93.5 ± 9.1	0.0	0.0	0.0	19.0 ± 4.9	11.0 ± 4.3	60.6 ± 5.5
Membrane	3.3 ± 5.8	3.3 ± 5.8	0.0	0.0	7.9 ± 15.8	6.5 ± 9.1	100	100	100	22.8 ± 17.6	78.4 ± 18.4	46.6 ± 11.9

[a] Values are means ± standard deviations of three different determinations.

Purification and characterization of processed cytochrome b_5 from the tb5wt transformant

Since the processed product in the tb5wt transformant was shown to be localized in the periplasm, it was very easy to extract the product with minimal contamination. As shown in Fig. 4, lanes 1 and 2, a repeated